CHALMERS

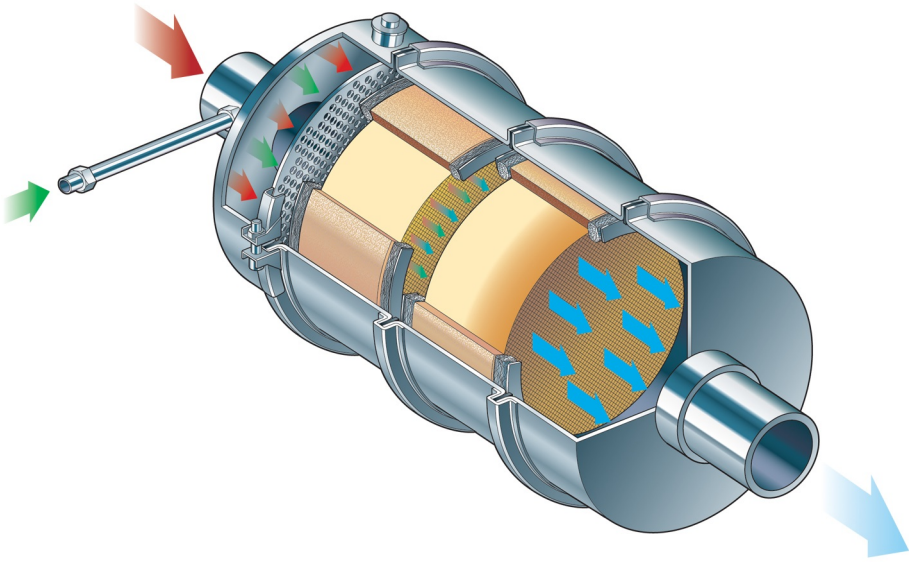

Ammonia Dosing Control Strategy for heavy duty automotive SCR

Master's Thesis in the Automotive Engineering

RAKSHITH RAMACHANDRA & SUDARSHAN RAMESH

Department of Applied Mechanics
Automotive Engineering
Chalmers University of Technology
Gothenburg, Sweden 2014
Master's Thesis 2014:69

Abstract

Selective Catalytic Reduction (SCR) has proven to be the frontrunner for the removal of nitrogen oxides (NO_X) from exhaust gas. EURO VI emission regulations present a challenge from the control point of view, so as to achieve high NO_X conversion while keeping the ammonia slip under control. This thesis focuses on a model based feedforward control system to dose the urea. The SCR is modeled as a series of CSTR (continuously stirred tank reactor) with the main SCR chemical kinetics. The main reactions are ammonia adsorption, desorption, fast SCR, slow SCR, standard SCR and ammonia oxidation. The model is simplified so as to capture the important dynamics and be fast at the same time. A fast and computationally less demanding model is required from a control aspect if it has to be implemented online.

Two control strategies were evaluated. The first control strategy maintains a constant ammonia slip whereas the second controller maintains a constant NO_X to ammonia ratio at the outlet of the SCR.

The catalyst used is an extruded vanadia based catalyst. The control strategy was tested on the engine bench with a 11.4L catalyst and an inline 6 cylinder 12.8L engine. The performance of the controller was very good compared to a flat urea dosing. The control strategy achieves a higher NO_X conversion, less ammonia slip and uses less urea for injection.

KEYWORDS: SCR modeling, SCR control, Selective catalytic reduction modeling, SCR catalyst modeling, urea scr catalyst modeling, urea scr catalyst control, ammonia dosing control, physics based SCR model

Acknowledgements

The thesis was carried out at Johnson Matthey technical center, Göteborg, Sweden. We would like to express our gratitude to Mr. Jonas Edvardsson, HD Applications Engineer, Johnson Matthey for his support throughout the entire six months. His assistance in the modeling of the SCR has been very valuable. We would also like to thank Dr. Jonas Sjöblom who is the co-supervisor for this thesis. Without his assistance in design of experiments and parameter estimation getting a working model would not have been possible.

We would also like to extend our gratitude to Mikael Larsson for allowing us to do our thesis at Johnson Matthey. Finally we thank the test engineers Anders Sääw and Nils Västgöte at the test cell without whose help we could have not validated the performance of the controller.

We thank our respective universities for allowing us to go an Erasmus exchange studies to ETH Zürich for a semester. A special thanks to Dr. Christopher Onder for handling the course on 'Engine System Modeling and Control'. This course served as the basis for modeling and control of the SCR system.

Last but not the least we would like to thank our families for providing us the opportunity to study in Sweden. The experience has been wonderful.

Sudarshan Ramesh, Rakshith Ramachandra, Göteborg 2/6/14

Contents

Nomenclature

A	Area [m^2]
A_i	Experimentally determined constants for temperature dependent specific heat capacity of exhaust gas
ANR	Ammonia to NO_X ratio
BSFC	Brake specific fuel consumption [g/kWh]
C_i	Gas phase concentration of species i [mol/m^3]
C_p	Specific heat capacity at constant pressure [J/kg K]
C_s	NH_3 adsorption capacity [mol/m^3]
D	Diameter [m]
DDR	Double data rate
E_a	Activation energy [kJ/mol]
ELR	European load response cycle
ESC	European steady cycle
ESC R-49	Urban driving cycle
ETC	European transient cycle
F_v	View factor
h	Heat transfer coefficient [W/Km^2]
J	Optimization criteria or cost function
k	Pre-exponential factor [s^{-1}]
L_v	Latent heat of vaporization [J/kg]
LHV_{Diesel}	Lower heating value of diesel=42.5 [MJ/kWh]
M_i	Experimentally determined constants for temperature dependent specific heat capacity of the catalyst substrate
m	mass [kg]
$\dot{m}$	Mass flow rate [kg/s]

$N_{cell,T}$ Number of cells for the temperature model

N_{cell} Number of cells in the model

n Moles [mol]

$\dot{n}$ Molar flow rate [mol/s]

P Pressure [Pa]

Q Heat capacity [J]

$\dot{Q}$ Heat flux [J/s]

R Universal gas constant [J/mol K]

$R_{ex.gas}$ Gas constant of exhaust gas [J/kg K]

r Rate of a reaction [mol/m^{3}s] (In terms of void volume)

RAM Random access memory

T Temperature [K]

V Volume [m^3]

WHTC World harmonized transient cycle

α Constant for surface coverage dependence of activation energy

γ Fraction of urea in AdBlue

ϵ Void fraction expressed as a ratio of open volume of the convertor /total volume of the convertor

ϵ_{rad} Emissivity

η Engine efficiency

θ Fraction of ammonia adsorbed on the catalyst surface [-]

$\dot{\theta}$ Rate of change of fractional surface coverage

σ_{SB} Stephen-Boltzmann constant [W/m^2 K^4]

1

Background

This section will briefly explain how NO_X is formed during combustion, why NO_X emissions must be reduced and the harmful effects associated with NO_X emissions.

The three primary sources of NO_X in combustion processes are:

- Thermal NO_X
- Fuel NO_X
- Prompt NO_X

During the combustion process in an internal combustion engine, most of the NO_X formed is thermal NO_X[1]. The formation of thermal NO_X is explained by Zeldovich mechanism. During very high temperatures the rate of formation NO is higher. If given sufficient time the equilibrium concentration is reached. But in an IC engine during the expansion stroke the temperature drops drastically hence large amount NO_X formed during the high temperatures does not reach the equilibrium state. Such a state is referred to as a frozen state.

Fuel NO_X is formed when nitrogenous compounds in the fuel react with oxygen. Gasoline and other distillates have no nitrogen bound compounds in the fuel, hence NO_X formed due to this process can be neglected [1].

Prompt NO_X is formed when the hydrocarbons in the fuel react with nitrogen to form intermediates such as HCN and H_2CN during the early stages of combustion. These later oxidise to NO. Once again the contribution of prompt NO_X to NO_X emissions is minimal [2]. Essentially most of the NO_X formed during combustion process is due to thermal NO_X [1].

Why is NO_X harmful?

- Health hazard: NO is poisonous and an irritant. It can cause headache and nausea. Long exposures can cause suffocation and cyanosis. NO_2 is toxic and an irritant. It can cause pulmonary edema [3].
- Environmental effects: NO_X in the presence of sunlight and organic compounds reacts to form ozone. Ozone in the troposphere is called ground level ozone. NO_X can combine with water to form nitric acid which causes acid rain [4].

Due to the above mentioned effects on humans and environment NO_X emissions has to be reduced.

2

Introduction

Selective Catalytic Reduction (SCR) is used to reduce the oxides of nitrogen which are NO and NO_2 to N_2 and H_2O. The use of this system to reduce NO_X emissions has been in place since a long time. It was patented in the United States by the Engelhard Corporation in 1957 [5].

SCR technology was implemented on a commercial vehicle to meet the EURO IV regulation [6]. Since then the use of SCR in automotive applications has been increasing. There are other technologies such as EGR (Exhuast Gas Recirculation) and LNT (Lean NO_X trap) which are used to reduce the NO_X emissions. EGR reduces the NO_X emissions by diverting a part of the exhaust back into the cylinder. As this recirculated combusted gas is inert it lowers the adiabatic flame temperature in the cylinder. Lowering the adiabatic flame temperature reduces the amount of NO_X formed.

LNTs work by adsorbing the NO and NO_2 molecules on the surface. Once the catalyst is full it must be regenerated. This is typically done by injecting fuel and burning it. The hydrocarbons in the fuel reduce the NO and NO_2 to N_2 and H_2O.

Both the LNT and EGR systems impose a penalty on the fuel consumption. The use of additional fuel in the LNT system is seen clearly by the use of diesel to reduce the NO_X. In the EGR system, lowering the adiabatic flame temperature lowers the efficiency which leads to increased fuel consumption.

The SCR system is popular because the engine can be tuned to operate at a very high efficiency which implies higher flame temperatures without compromising the NO_X conversion. There are combinations of EGR+SCR, pure SCR and pure EGR which have been used in the past. For EURO VI and above emission regulations SCR+EGR and SCR only solution are viable options to reduce NO_X without compromising on the engine efficiency. FPT were the first to introduce an SCR only solution [7]. Since then a number of other manufactures like Scania have opted for the SCR only option [8]. A more detailed comparison of SCR, SCR+EGR and EGR only solution to meet Euro VI emission regulations was conducted by TNO [9].

The EURO VI emission regulations came into effect form the Jan 1st 2014 for heavy duty vehicles. The regulation places a stringent limit on tail pipe NO_X emissions. The EURO VI regulations require the tail pipe NO_X to be under 0.4 g/kWh, PM(Particulate matter) 0.01 g/kWh while the average ammonia slip must be below 10 ppm with a 50 ppm peak slip limit [10]. The US 2010 regulations place a more stringent limit on the NO_X emissions. It requires the NO_X emissions to be under 0.26 g/kWh. Moreover the emissions from the cold and hot cycle are weighed and then the total emission is calculated. At present the weight for the cold cycle is 0.1 and for the hot cycle is 0.9. These limits necessitates for a good control strategy to achieve high NO_X conversion

and limit the ammonia slip. Anhydrous ammonia is very toxic, highly irritating gas with sharp, suffocating odor. The pungent odor becomes noticeable from about 5-10 ppm hence the regulation to control the ammonia slip [11]. Controlling the ammonia slip will require clever control strategies and traditional method of dosing at flat ANR (Ammonia to NO_X ratio) cannot be used anymore. The SCR has side reactions which involve formation of N_2O and other species. Future emission regulations might place a limit on these emissions as well.

The reducant is dosed in the form of an aqueous urea solution, called as AdBlue in Europe and DEF (Diesel exhaust fluid) in North America. AdBlue is an aqueous urea solution containing 32.5% pure urea and 67.5% deionized water [12]. This is a eutectic solution which means that this composition has the lowest freezing point compared to any other composition. This lowers the freezing point of urea which is helpful in cold driving conditions. Anhydrous ammonia is not used for automotive applications as it is highly toxic which makes handling and storage onboard tricky. Typically the urea solution is dosed upstream of the SCR where it mixes with the hot exhaust gas and undergoes thermolysis and hydrolysis to form ammonia. This ammonia adsorbs on the catalyst surface and reacts with the nitrogen oxides to form nitrogen and water.

2.1 Comparison of SCR, EGR and LNT

This section will give introduction into the various technologies that are currently available for the reduction of NO_X emissions. The technologies in place are namely SCR, EGR and LNT. SCR so far has been used only for heavy duty applications. With new regulations SCR will be implemented on light duty vehicles. LNT so far has been applicable only for light duty vehicles.

2.1.1 SCR

SCR stands for selective catalytic reduction. SCR catalysts remove nitrogen oxides (NO_X) using a reducing agent ammonia (NH_3). A SCR catalyst is used to speed up the reactions and to provide a surface on which the reactions take place. As mentioned earlier the reducing agent is carried on board the vehicle as an aqueous solution containing 32.5% urea. This solution is called AdBlue and is used as the storage and transportation is easier, moreover it is dangerous to carry anhydrous ammonia onboard.

The dosing system consists of the tank to store the AdBlue, pump, and an injector. In addition ot these there can be a dosing control module if the system is not controlled by the ECU. Currently there are two technologies available for dosing: Air assisted systems and airless systems. In the air assisted system compressed air is used to get a fine spray of reducing agent through the injector, whereas in the airless system the reducing agent itself is compressed. The urea injected is converted to ammonia through the process of thermolysis and hydrolysis.

The standard SCR layout for a heavy duty vehicle looks as shown in the figure 2.1. In addition to the SCR there can be an ASC (Ammonia Slip Catalyst) downstream of the SCR. The function of the ASC is to oxidise the ammonia slip from the SCR.

The SCR is most efficient between a temperature range of 200 and 400 °C. At lower temperatures the SCR kinetics is slow which limits the NO_X conversion and in addition at lower temperatures it is difficult to decompose the AdBlue solution. At temperatures greater than 400 degrees ammonia oxidation kinetics become more important a larger part of the ammonia gets converted to N_2 and NO_X which is detrimental to NO_X conversion as there is no ammonia to reduce the NO_X.

It was possible to achieve NO_X conversion of upto 90% by using EGR (Exhaust Gas Recirculation) and some optimization of the engine. The use of SCR became dominating with the

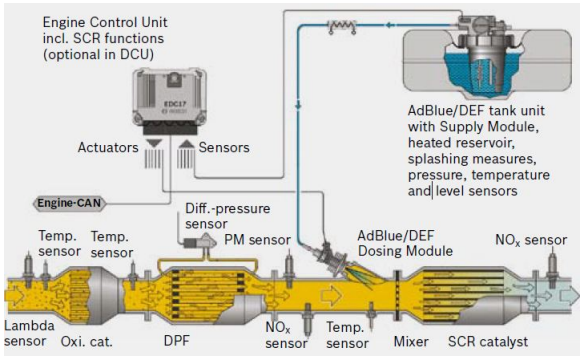

Figure 2.1: SCR layout in a heavy duty vehicle. Consists of the DOC(Diesel Oxidation Catalyst), DPF(Diesel particulate filter), Urea injector, SCR [13]

implementation of EURO VI emission regulations. The emission regulation trend curve can be seen in Figure 2.2.

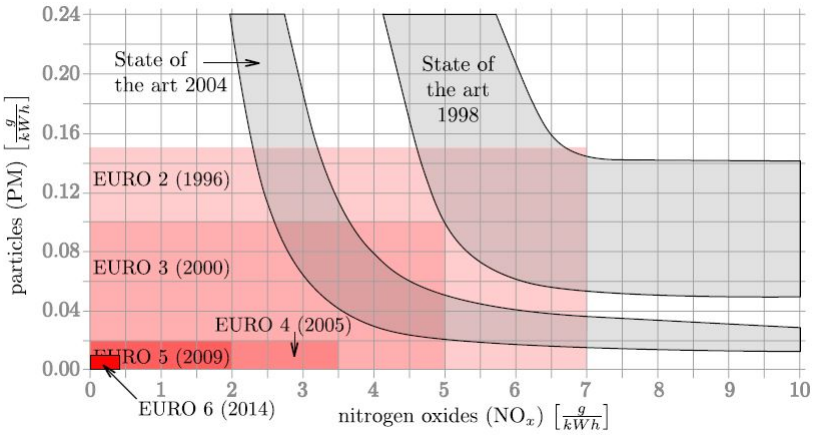

Figure 2.2: Legislative limits and trade off of raw emissions for heavy duty diesel engines : Particulate matter vs NO_X [14]

.

As seen from the figure 2.2 EURO VI regulations places a tough limit on both the PM and NO_X emissions. The grey region takes into effect of deterioration system performance such as catalyst ageing. Therefore when the system is designed the lower curve of the grey region is the bench mark and with time due to ageing and other factors it would be the upper curve of the grey region. This figure also shows the typical 'Diesel Dilemma' which is the trade-off between NO_X and particulates. A higher PM would mean lower NO_X and vice versa. The EGR solution increases the PM while reducing the NO_X, the capability of this system is at the limit if the efficiency of the engine is also to be considered. The advantages of using the SCR solution are clear.
The advantages are : 1. Higher specific power output 2. Improved engine life and efficiency 3. Increased reliability 4. Lower cost of operation [15].

The increase in fuel efficiency, without considering the usage of AdBlue can be anywhere between 4-5% [16] when compared to EGR+SCR solution. The fuel efficiency is higher because the engine can be optimized to operate at a high efficiency point. This high efficiency point corresponds to higher combustion temperatures which lead to higher NO_X formation. The NO_X is treated separately using the aftertreatment system which in this case is the SCR. Secondly the frequency of regeneration of particulate filter is lower now as the PM is reduced due to a more efficient combustion process. This in turn saves more fuel but of course the cost of AdBlue usage must be considered for calculating the operating costs. With an SCR only system the AdBlue usage increases.

2.1.2 EGR

EGR stands for exhaust gas recirculation. In this process a portion of the exhaust gas is diverted back to the intake where it is mixed with the fresh intake air and fed into the cylinder for combustion. The process by which the EGR has an influence on reducing the NO_X is by two ways: 1. Due to the presence of the inert recirculated exhaust gas in the intake air, the specific heat capacity of the mixture is higher. This lowers the adiabatic flame temperature which leads to lower NO_X formation during the combustion process. 2. The oxygen content per unit volume of intake air is lowered hence the NO_X formation is reduced.

An EGR system employed in a diesel engine can be mainly of two types: 1. LP (Low Pressure) EGR 2. HP (High Pressure) EGR . The schematics of these two systems is depicted in the figure 2.3 [17]. In the LP EGR system the exhaust gas from the downstream of the turbine is connected to the to the upstream of the turbocharger. In the HP EGR system the exhaust gas from the upstream of the turbine is connected to the downstream of the compressor. A HP EGR system helps to increase efficiency by reducing the pumping work.

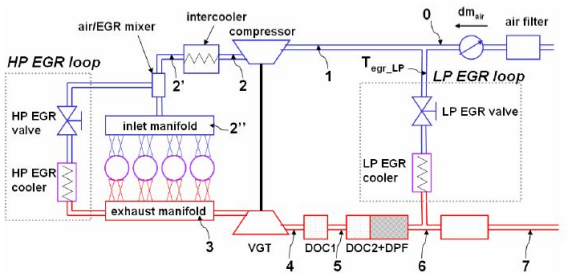

Figure 2.3: Low pressure and high pressure EGR schematics. [17]

Though EGR helps to reduce NO_X it has some disadvantages. One of the main drawbacks of using EGR is increase in the PM (Particulate Matter) emissions this indirectly affects the efficiency as the most of the PM is unburnt HC and soot. This is the main reason why EGR only solution is not capable of meeting the future emission regulations. The second drawback is that the DPF (Diesel particulate filter) needs to be regenerated more often. This is due to increased soot production which adds to the fuel penalty as the regeneration is performed by injecting fuel and burning off the soot. Thirdly the life of the engine comes down due to the presence of particulates which increases the wear and blowby. Increased blowby leads to contamination of the engine oil.

2.1.3 LNT

LNT stands for lean NO_X trap. As the name suggests it traps the oxides of nitrogen. The LNT consists of three active components: 1. Oxidation catalyst - platinum 2. Adsorbent - barium 3. Reduction catalyst - rhodium [18]. During lean operation NO from the engine and the oxygen in the exhaust react on the surface in the presence of Pt catalyst to form NO_2. The NO_2 formed is adsorbed by the storage material in the form of barium nitrate. When the adsorbent is saturated with NO_2 the system must be regenerated. The regeneration is done by switching to rich operating conditions. The oxides of nitrogen are reduced to N_2 over the reduction catalyst. Like the EGR, LNT imposes a fuel penalty as the LNT needs to be regenerated.

The process is shown in a schematic form in figure 2.4.

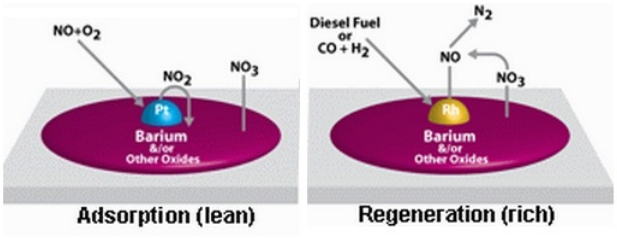

Figure 2.4: Adsorption and reduction process in an LNT. [18]

2.2 Scope of the master thesis

As a part of this thesis, a control strategy is developed in order to achieve high NO_X conversion levels while restricting the ammonia slip at the outlet of the SCR. The main goal is to develop a model-based feedforward control strategy which shows good performance for different test cycles and which can be implemented for future use. The first step is to analyse the chemical kinetics of an SCR system and build a mathematical model of the system. Once the model is built and the various parameters of the model are estimated through an optimization routine. For this purpose the output from a detailed kinetic model is used. Once the parameters are estimated, the model is validated by using measurement data.

This is followed by the development of two model-based feedforward control strategies. One is used to maintain a constant ammonia slip while the other is used to maintain a constant NO_X/NH_3 ratio. Both the controllers are validated on an engine bench for a certain catalyst volume by running the engine through the WHTC cycle. The results are then compared to a flat ANR dosing strategy. Finally, suggestions are made for improvements and future work that can be carried out in this area is discussed.

2.3 Objectives of the project

The goal of the thesis project was to develop and evaluate control strategies for a different catalyst formulations developed by Johnson Matthey. The objectives of this project are:

- Develop an SCR model for an extruded vanadia catalyst formulation. The model can be used for other catalyst formulations as well. Any additional reactions which are deemed relevant for later use can be added to the model as well.
- Use a detailed kinetic model provided by Johnson Matthey AB to estimate various chemical reaction parameters as well as the NH_3 storage of the catalyst. The detailed kinetic model is also used to validate the performance of the SCR model by using engine-out NO_X emissions for various test cycles.
- Build a feedforward controller using the SCR model. The controller is built for offline use and to generate AdBlue dosing profiles by using engine-out NO_X emissions for specific test cycles.
- Validate the performance of the feedforward controller for the by using the dosing profiles generated on the engine bench.

3

Literature review

This section provides an overview of the literature review carried out with respect to SCR including the aspects of modelling and control. To gain a basic understanding of the chemistry involved in SCR systems, a thorough literature review was carried out related to the concepts of surface chemistry, collision theory as well as chemical kinetics. References [19],[20] were referred to gain an understanding of the concepts of surface chemistry and chemical kinetics. Literature related to modeling and control of SCR systems was found in [21] and [22].

From the literature review a good understanding of the modelling of an SCR system was gained. The methods adopted in literature for the modelling of SCR systems have also been adopted for our thesis. Various control strategies for the control of SCR systems have been developed over the years in order to bring down NO_X emission levels. These control strategies also aim to limit the emission of NH_3. Some of the control strategies used are presented below:

3.1 Control strategies

1. **Feedforward control of SCR systems** For a feedforward control strategy, usually a map-based or model-based system is in place. In case of a map-based system, the output of the controller which should be the amount of urea to dose is usually obtained from a look-up table. The amount of urea to be dosed is found in the look-up table for each engine operating point. The map based system is usually developed for the steady-state operation of the SCR system [23]. As per Willems et. al [24] [23] an open loop control system is sufficient to meet Euro 4 and Euro 5 emission standards. However, the performance of a map-based system is not very accurate during transient tests. The EU emission norms for different tailpipe out emissions are shown in tables 3.1 and 3.2.

   During the course of this thesis a map based system was tested for the World Harmonized Test Cycle (WHTC). It was observed that the map based system did not really achieve any significant reduction in NO_X emission and ammonia slip compared to a system with a flat dosing of ammonia to NO_X ratio (ANR).

   To meet Euro VI emission standards which demand a significant reduction in emissions relative to Euro 5, a model based system will be required. A model-based open loop control system has very good performance even during transients. A model-based system usually consists of a simple model of the SCR system incorporating the chemical kinetics and a temperature model. In this thesis, a model-based feedforward only approach has been considered.

Table 3.1: EU emission norms for heavy-duty diesel engines (Steady state testing). (* - PM=0.13 g/kWh for engines < 0.75 dm^3 swept volume per cylinder)

Stage	Date	Test	CO [g/kWh]	HC [g/kWh]	NO_X [g/kWh]	PM [g/kWh]
Euro I	1992	ECE R-49	4.5	1.1	8.0	0.612
Euro II.a	Oct. 1996	ECE R-49	4.0	1.1	7.0	0.25
Euro II.b	Oct. 1998	ECE R-49	4.0	1.1	7.0	0.15
Euro III (EEV Only)	Oct. 1999	ESC and ELR	1.5	0.25	2.0	0.02
Euro III	Oct. 2000	ESC and ELR	2.1	0.66	5.0	0.10*
Euro IV	Oct. 2005	ESC and ELR	1.5	0.46	3.5	0.02
Euro V	Oct. 2008	ESC and ELR	1.5	0.46	2.0	0.02
Euro VI	Jan. 2013	ESC and ELR	1.5	0.13	0.4	0.01

Table 3.2: EU emission norms for heavy-duty diesel engines (Transient testing). (* - PM=0.21 g/kWh for engines < 0.75 dm^3 swept volume per cylinder)

Stage	Date	Test	CO [g/kWh]	HC [g/kWh]	NO_X [g/kWh]	PM [g/kWh]
Euro III (EEV Only)	Oct. 1999	ETC	3.0	0.4	2.0	0.02
Euro III	Oct. 2000	ETC	5.45	0.78	5.0	0.16*
Euro IV	Oct. 2005	ETC	4.0	0.55	3.5	0.03
Euro V	Oct. 2008	ETC	4.0	0.55	2.0	0.03
Euro VI	Jan. 2013	WHTC	4.0	0.16	0.46	0.01

A schematic diagram of a feedforward control system is shown in figure 3.1.

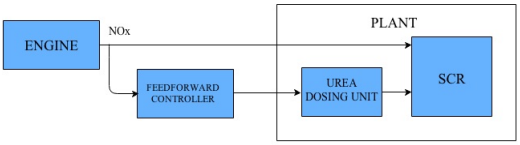

Figure 3.1: Schematic diagram of a feedforward control system

2. **Feedback control of SCR systems**

Traditional feedback control systems includes a PID controller which is used to control the urea dosing to the SCR. A schematic of such a system is shown figure 3.2.

The feedback controller is mainly used to account for:

- Inaccuracy in modelling. One of the challenges of using feedback information from the NO_X sensor downstream of the SCR is the cross-sensitivity to NH_3. A sensor is said to be cross-sensitive when it detects other gases along with the gas concentration it is

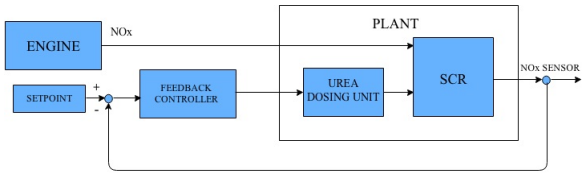

Figure 3.2: Schematic diagram of a conventional feedback control system

supposed to measure. Most commercially available NO_X sensors are also sensitive to NH_3 leaving the catalyst and this can cause an error in the measurements. This can make the feedback loop unstable. To account for this, a cross-sensitivity compensation is applied.

- To make the control system more robust.
- To account for reduced catalyst activity due to catalyst aging.

3. **Advanced control strategies**

Recent literature in the area of SCR control e.g [25] and [26] focus on optimizing the control system. B Hollauf et al. propose a control strategy wherein they focus on obtaining an optimal NH_3 loading set-point for various operating conditions. By NH_3 loading on the SCR catalyst, one means injecting sufficient urea a to store a sufficient amount on the catalyst surface. This setpoint is optimized for various operating conditions by considering a trade-off between the NO_X conversion and NH_3 slip desired.

Other advanced control strategies such as model predictive control have also been proposed in literature. For e.g. McKinley et al. propose a model predictive control strategy in [27]. In a model predictive controller, the model used is detailed and is used to predict the output of the system over a future time horizon. The control output is chosen so as to minimize a certain cost function. The main advantage of model predictive control is that all the required constraints are taken into account when the control output is determined. The main disadvantage of this system is that an optimization routine needs to be carried out at each time step which can increase the computational time. However with increasing power of microprocessors, model predictive control has a very high potential for future applications.

Stevens et al. propose an optimized control strategy wherein the urea dosing profile is optimized for various operating conditions. Using optimal control to obtain the desired emissions is to go a step further towards the development of better control strategies. However, optimization is sometimes used to develop a strategy suited for a specific driving cycle. A driving cycle is used in order to test a system on real-world driving conditions. It was discovered in a study by the World Health Organization that auto manufacturers engaged in a practice where the engine performance was optimized for a specific drive cycle [28]. The the emissions of the vehicles would be much higher in a real driving conditions than during a test cycle. This compromises the performance of the aftertreatment system in regular driving conditions. This needs to be avoided because it leads to poor emission standards and also higher emissions which can be a cause for pollution related health issues. Control strategies that can handle all kinds of drive cycles are needed. However the primary focus of legislators and engine manufacturers is to comply with in use needs and not to meet just drive cycle requirements.

3.2 SCR chemical kinetics

This section provides a brief overview of how SCR systems are generally modelled. A detailed description of the modelling of SCR systems will be provided in the next section of this report.

Models of SCR systems generally comprise of the following sub-models:

3.2.1 SCR kinetic model:

The NH_3 storage model consists of modelled reaction rates. These reaction rates are used to calculate the gas phase concentrations of NO_X as well as NH_3. Detailed kinetic models such as the ones used by catalyst manufacturers such as Johnson Matthey and BASF are very detailed. They usually include the reaction rates of all the reactions that occur or certain side reactions that might occur inside an SCR convertor.

For control purposes, the chemical reactions are selected depending on which reaction is considered to be the most significant. Some SCR models seen in ex.[21] and [22] model only some of the reactions which the authors consider to have the maximum impact on the emissions. This is done to ensure that the model is simplified but captures all the relevant emissions at the same time. This also ensures that the model runs relatively quickly. These models are also modelled based on certain simplifying assumptions [29]:

- As a one-dimensional model where the variables are considered to vary only along the direction of flow [21]. This is done in order to avoid partial differential equations. The SCR monolith is considered to be made up of a number of continuously stirred reactors in series. The model only models only one channel. Any radial effects over the substrate are ignored.
- Side reactions that produce N_2O as well as the oxidation of NH_3 to NO are neglected in these models. This is because these side reactions are not considered to have a significant impact on the outlet emissions of NO_X from the SCR.
- The hydrolysis and thermolysis of AdBlue is neglected. Any wall wetting dynamics of AdBlue in the pipe is also not considered to be significant. All the AdBlue is assumed to decompose into urea. One mole of urea forms two moles of ammonia.
- The gas entering the SCR system is considered to be ideal.

Tests are run on engines using specific SCR systems and the model parameters are identified using an optimization procedure. These models are specific to the type of catalyst used. E.g. for a set of parameters identified for an extruded vanadia catalyst cannot be used for a Cu-Zeolite catalyst as the reaction kinetics differ depending on the substrate and washcoat of the catalyst.

Chemical kinetics in an SCR system

The chemical kinetics in an SCR system involve the following reactions:

1. **Adsorption and desorption of NH_3 onto the surface of the catalytic convertor**:

   This mechanism can be depicted by the following reaction:

   $$NH_3(g) + S \longleftrightarrow {NH_3}^* \tag{3.1}$$

   where S in equation 3.1 denotes a free site on the surface of the catalytic convertor and ${NH_3}^*$ denotes an ammonia molecule adsorbed onto the surface of the catalytic convertor. A free site on a catalytic surface is an empty void. This is formed due to the adsorbent (the coating of the catalytic convertor in this case) not being completely surrounded by the other adsorbent atoms [30].This empty site is occupied by the ammonia molecules. The forward reaction in equation 3.1 denotes adsorption of the ammonia molecule while the reverse denotes desorption of ${NH_3}^*$molecule.

   The adsorption of NH_3 on the surface of the catalyst is described by isotherms [30].These isotherms can be used to describe the concentration of the adsorbate (NH_3) on the surface of the catalyst as a function of the concentration [30]. According to [21] and [31] the Eley-Rideal mechanism is favoured for temperatures above 200 °C and the mechanism dominates

for temperatures above this temperature. The temperature of the exhaust gas from a diesel engine is generally above the temperature of 200 °C and thus the Eley-Rideal mechanism can be assumed to be the dominating mechanism for the SCR system.

2. **SCR reactions**

   There are mainly three important chemical reactions that occur beween the ammonia stored in the catalyst and the NO_X entering the catalyst.

   The first SCR reaction is called the *standard SCR*. This reaction is depicted below:

$$4\,NH_3 + 4\,NO + O_2 \longrightarrow 4\,N_2 + 6\,H_2O \tag{3.2}$$

   This reaction is important for NO_X conversion because around 95 % of NO_X out emissions from a diesel engine is NO.

   Another important SCR reaction is called the *Fast SCR*. This reaction is depicted below:

$$4\,NH_3 + 2\,NO + 2\,NO_2 \longrightarrow 4\,N_2 + 6\,H_2O \tag{3.3}$$

   Equation 3.3 consumes one mole of NH_3 per mole of NO_X and is faster compared to the standard SCR [14]. The diesel oxidation catalyst (DOC) alters the ratio of NO/NO_2. The ratio of NO/NO_2 in the engine out NO_X will thus change after the DOC. This will ensure that a major portion of the NO_X gets converted through the fast SCR reaction. The fast SCR is usually the dominant reaction when the ratio of NO/NO_2 is close to one.

   The last SCR reaction is called the *Slow SCR* and is shown below:

$$4\,NH_3 + 3\,NO_2 \longrightarrow \frac{7}{2}N_2 + 6\,H_2O \tag{3.4}$$

   The slow SCR reaction is usually not relevant as it can be neglected [21] . The reaction rate of the slow SCR becomes significant when all the NO is consumed inside the catalytic convertor.

3. **Ammonia oxidation reactions**:

   The oxidation of NH_3 needs to be considered during modelling as well. This is because the oxidation of NH_3 becomes significant at temperatures above 300 °C where it oxidizes to form N_2. This reaction is depicted below:

$$4\,NH_3 + 3\,O_2 \longrightarrow 2\,N_2 + 6\,H_2O \tag{3.5}$$

   The oxidation of NH_3 can also produce N_2O which is depicted below:

$$2\,NH_3 + 2\,O_2 \longrightarrow N_2O + 3\,H_2O \tag{3.6}$$

   This reaction is undesirable as it leads to the formation of N_2O.

   There are additional side reactions that occur inside an SCR convertor which are not deemed to be significant in this project and will not be discussed in this report.

The reaction rates of all these individual reactions modelled are used to calculate the ammonia stored inside the catalyst. Further explanation regarding the calculations involved will be provided in the next chapter of this report

3.2.2 Temperature model:

The SCR model also consists of a sub-model that calculates the temperature dynamics of the SCR system. The temperature model is based on simple heat balance. The SCR is assumed to be a perfect heat exchanger. This implies that the temperature exhaust gas leaving the SCR is equal to the temperature of the SCR. The SCR is assumed to be very well insulated therefore convective and radiative losses are ignored.

Some temperature models include conduction along the length of the SCR. The conduction effects have been ignored in this thesis. The temperature model described in [14] will be used for this thesis. Details of the temperature model adopted for this thesis will be provided in the next chapter.

3.3 Test cycles

Emission regulations in Europe are called as Euro emission norms. These emission legislations are formulated for different vehicle categories. In this section, the current Euro emission norms for trucks will be described in brief along with the test cycles used to evaluate the tailpipe emissions from heavy-duty truck engines.

Over the years, the European regulations for emissions have become stricter demanding better treatment of engine out emissions. To meet the current Euro VI norms, advanced aftertreatment systems are necessary along with efficient control strategies which keep the emission within the legislated limits.

Generally, the type of aftertreatment system chosen depends on the type of engine calibration. For e.g. if the engine is calibrated such that it it produces very low particulate emissions, a high efficiency NO_X conversion system needs to be in place.

There are standardized test procedures for heavy-duty truck engines along with specific after treatment systems in order to ensure that they meet the regulations. These test procedures involve the testing of the engine on various test cycles. These test cycles are carried out on an engine dynamometer.

Some of the common test cycles that have been used for emission norms are listed below [10]:

1. **European transient cycle (ETC)**:

   The European transient cycle was introduced in the year 2000 for emission certification purposes by the European commission. This cycle was developed by the former FIGE institute at Aachen, Germany based on real road test data for heavy-duty vehicles. This cycle is composed of the following three parts:

   - City driving with a maximum speed of 50 km/h. This portion of the drive cycle includes the frequent starts, stops and idling.
   - The second part of the drive cycle includes a portion for rural driving with an average speed of 72 km/h.
   - The third segment of includes highway driving with an average speed of 88 km/h.

   The length of each part is 600 s. The final emissions are expressed in g/kWh. Figure 3.3 represents speed and torque profiles of the ETC. [32]:

2. **European steady cycle (ESC)**:

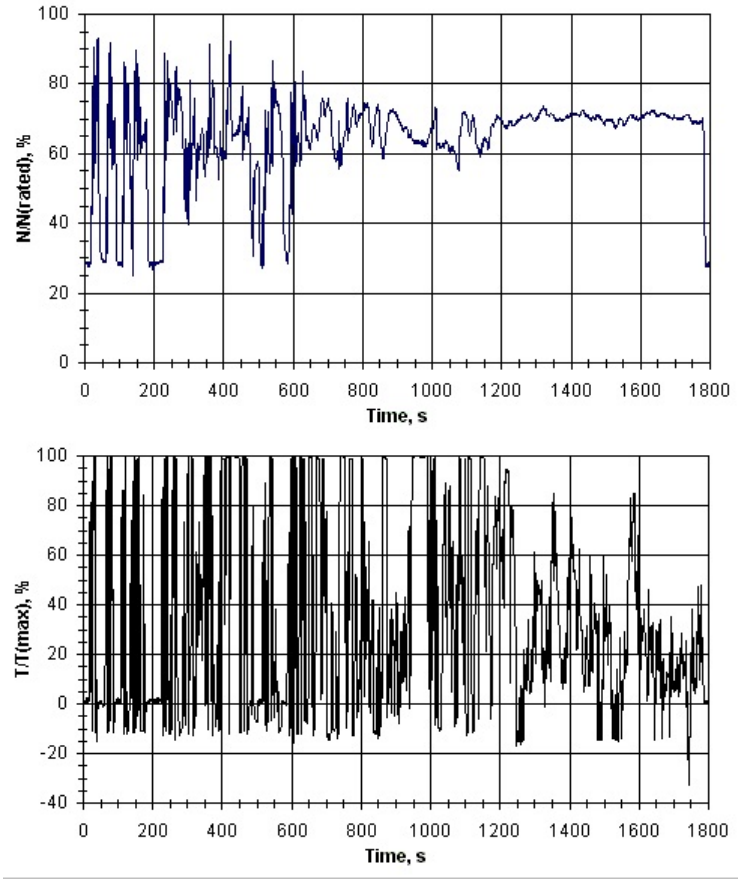

Figure 3.3: The European transient cycle - Speed and torque profiles [33]

The European steady cycle consists of 13 steady state operating modes and 3 random modes [34]. These modes cover the entire operating range of diesel engines. While running in the random modes, only the NO_X emissions are measured. The emissions from the engine are measured during each mode and averaged over the entire cycle. The final emissions are expressed in g/kWh. The total length of the cycle is 1680 s. High exhaust gas temperatures and high loads are characteristic of this cycle [33]. Figure 3.4 shows the various operating modes of the European steady cycle:

3. **World harmonized transient cycle (WHTC) and world harmonized steady cycle (WHSC)**:

   The WHTC and the WHSC cycles are test cycles that are defined by the global technical regulation introduced by the United Nations Economic Commission for Europe. Although different regulations for heavy-duty diesel engines were introduced in different countries, the measurement techniques used for emissions are different. To accurately analyse the effect of heavy-duty vehicles on the environment, a test cycle representative of the driving conditions in various parts of the world was introduced.

   The cycle is designed based on data representing typical driving conditions collected from the Europe, the United States, Australia and Japan. The WHTC cycle covers both cold start and hot start requirements while the WHSC is a steady state hot start cycle. This cycle was developed keeping in mind the applicability of the cycle to the existing after-treatment systems present at the time of introduction and also on the aftertreatment systems of the future. Another factor considered while designing the cycle was the applicability of the cycle to different heavy-duty engine types.

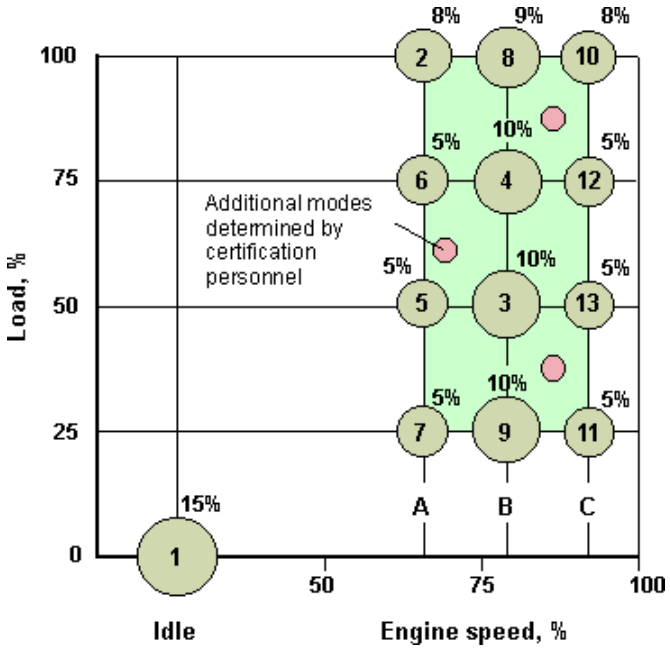

Figure 3.4: The European steady cycle for heavy-duty applications [33]

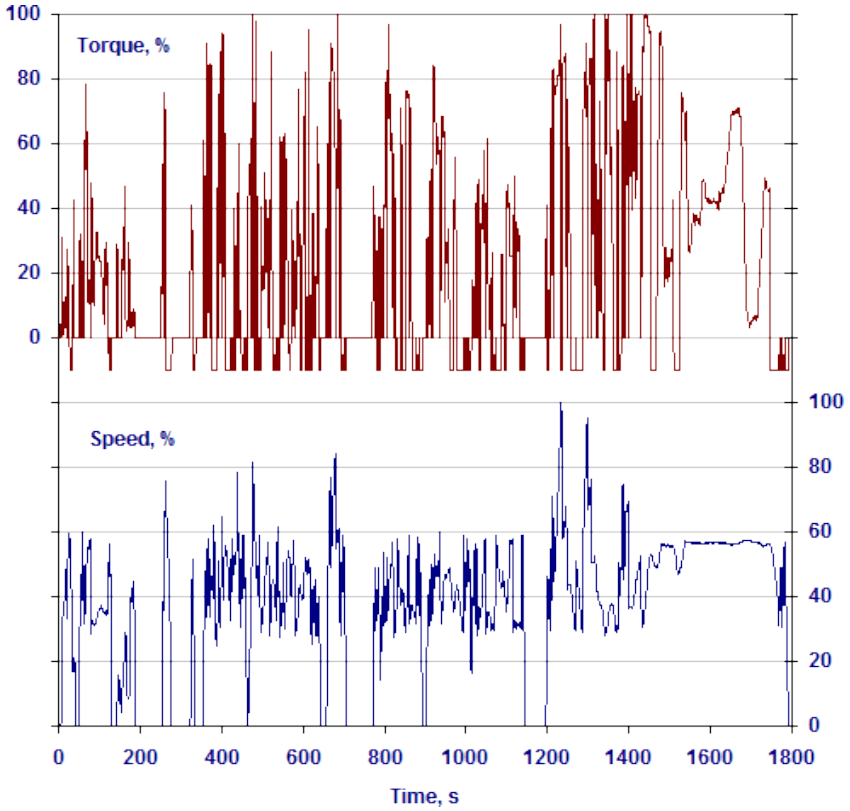

Figure 3.5: The world-harmonized transient cycle for heavy-duty applications [35]

The WHSC cycle is similar to the ESC cycle described earlier. It consists of 13 steady state operating modes. A weighting factor is assigned for the emissions from each mode. The overall emissions are averaged over the entire cycle using the weighting factors. The engine is operated in a particular mode for a designated amount of time before the speed and load are changed linearly.

3.4 Gas concentration measurement techniques

Various measurement techniques are employed in test benches to analyse the composition of the exhaust gas leaving the SCR. In this section the gas concentration measurement techniques employed for our tests will be described.

3.4.1 Chemiluminescence based exhaust gas analyzer

For the measurement of gas concentrations during tests carried out at the engine bench a Horiba MEXA-7100D exhaust gas analyser was employed. The analyzer measures NOX using the principle of Chemiluminescence. Chemiluminescence is a phenomenon where light is emitted due to a chemical reaction. For example in the Horiba MEXA-7100D, the concentration of NO is measured by reacting ozone(O_3) with NO. This reaction produces electronically excited NO_2 which emits a photon before reaching a ground state. This emitted radiation is monitored which gives a measure of the concentration of NO. The analyzer can measure NO_X, CO, CO_2, THC and O_2 [36].

3.4.2 Quantum cascade laser (QCL)

Quantum cascade lasers are semiconductor lasers which emit radiations in the mid to large wavelength infrared radiation band. QCLs are mainly used for measurement of gas composition. QCLs can be tuned to a wide range of wavelengths and can be used to measure gas species such as NH_3, NO_X, CO and CO_2. They can be used in place of traditional FTIR systems primarily because they are faster and are also smaller. However they currently expensive and are used primarily for specialized applications [37]. The QCL employed for the tests carried out as a part of this thesis is a Horiba MEXA 1400QL-MX. This analyzer uses a mid-infrared QCL and can be used to measure gas components mainly NO, NO_2, N_2O and NH_3 even in very small concentrations over a wide range.

3.5 Maldistribution of NH_3

Maldistribution of NH_3 at the inlet of the SCR can affect the chemical reactions occuring in the SCR and also affect the NH_3 slip occuring at the outlet of the SCR. Maldistribution of NH_3 due to improper mixing can lead to higher concentrations of NH_3 in some portions of the SCR and lower concentrations of NH_3 in other portions.

This can lead to poor overall NO_X conversion and a higher NH_3 slip. Thus ensuring good mixing is important. To determine uniformity of mixing, a term called uniformity index is used. A uniformity index of 1 indicates perfect mixing. The uniformity index was primarily used for velocity distributions but it can be applied to any property that one wishes to analyse at the inlet of the SCR convertor [38]. Variables that have a significant impact on the NO_X conversion and NH_3 slip such as ANR can be analysed using the uniformity index. The uniformity index can be expressed as

$$UI = 1 - \frac{1}{2.A_{SCR}}.\int_{A_{SCR}} (\frac{P}{P_{avg}} - 1).dA \tag{3.7}$$

where P is the parameters of interest.

To ensure good mixing of the NH_3 with the exhaust gas, mixers are used in the exhaust pipe. An image of a mixer is shown below:

The mixer shown in 3.6 is an example of a static mixer that is used in exhaust pipes before the SCR. Static mixers induce turbulence and facilitate better mixing. The mixer is usually placed between the urea injector and the SCR inlet. A mixer generally gives a higher pressure drop compared to a case without a mixer. Hence, important considerations when designing mixers for SCR systems are low pressure drop and good mixing [40].

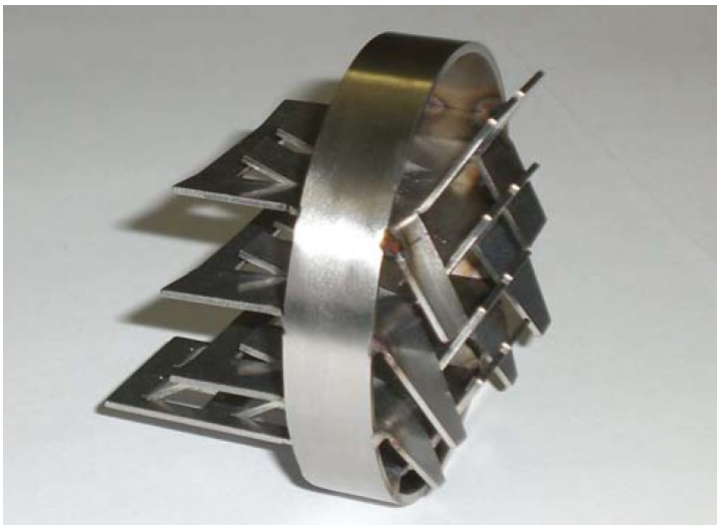

Figure 3.6: A 2-stage mixer for urea SCR application adopted from [39]

3.6 Carbon footprint of urea

The carbon footprint can be defined as the total greenhouse gas emissions that are produced by an organization, event or a product. Usually the sources of greenhouse gas emissions can be classified into direct and indirect sources. Usually, the majority of the greenhouse gas emissions occur due to indirect sources which are far away from the end consumer. Urea is one of the main components of AdBlue. Urea is produced on a large scale from liquid NH_3 and CO_2. Urea production actually has the potential to reduce one of the main greenhouse gases *i.e.* CO_2. This is because CO_2 is utilized directly in the production of urea. Over the past 50 years, the processes used to produce urea have also improved significantly which further reduce any emissions that may occur due to the manufacturing process.

Current manufacturing plants utilize less power and are more energy efficient. The CO_2 that is released to the atmosphere through flue gases and emissions from chemical plants can be utilized for urea production. Urea thus has a low carbon footprint at the production stage. However CO_2 emissions can occur when urea is used as a fertilizer for land application through hydrolysis in the soil. Urea is synthesized in liquid form also called as urea melt. The urea melt is mixed in a plant with demineralised water in the right proportions to form AdBlue [41].

The carbon footprint of urea is significantly influenced by the fuel used in the production process. Larger emissions are observed if coal is used for urea production compared to the case when natural gas is used. Fossil fuels such as coal and natural gas are mainly used for the steam reforming process used to produce hydrogen which in turn is used to produce NH_3 through the Haber-Bosch process. Natural gas is the most commonly used fossil fuel with approximately 80 % of the world's ammonia being produced using natural gas. Modern plants are equipped with systems to recover the supplementary CO_2 produced during the combustion of natural gas.

Emissions associated with the extraction, production and transmission of natural gas also contributes to the overall carbon footprint associated with urea production. Additional sources such as leakage during transportation also contribute significantly. With recent advances in production processes, the carbon footprint associated with urea production has decreased in the past decade. According to the international fertilizer association, the energy consumption for the urea production plants has decreased by 9% over the last decade. From an agricultural perspective, the carbon footprint associated with urea is larger. However from the point of view of AdBlue production, the carbon footprint is significantly smaller. The following table shows the emissions and energy use starting from the production of natural gas till the production of ammonia:

Table 3.3: Greenhouse gas emissions and energy consumption for the production of ammonia in different regions of the world (Adopted from [42])

Region	t CO_2/ t NH_3	MJ/ t NH_3
Western Europe	2.34	41.6
North America	2.55	45.5
Russia and Central Europe	3.31	58.9
China and India	5.21	64.3
Rest of the world	2.45	43.7
World average	3.45	52.8

3.7 Fuel penalty and costs associated with urea SCR

Urea SCR technology is a very promising aftertreatment technology. Not only does it allow a higher NO_X conversion on a wider temperature window, but it also has an insignificant fuel penalty associated with it. This is because the engine can be calibrated to operate at optimum fuel consumption rather than calibrating it to lower NO_X emissions. Thus the injection timing of the engine can be advanced. Although this has a negative impact on the NO_X emissions it has a positive impact on soot emissions and also improves fuel economy.

Compared to emission control technologies, SCR also has lower system cost and lower operating cost. Lambert et. al in [43] demonstrate the application of urea SCR technology for low and heavy duty vehicles and observe the costs associated with it. As a part of this study, the fuel penalty associated with LNT and SCR systems was observed. While LNT systems showed a fuel penalty of 7% to achieve a NO_X conversion of 80 %, SCR technology showed no direct fuel penalty. If fuel penalty associated with the production of urea was to be considered, it accounted for 0.2 %.The operating cost of LNT was observed to be almost 3 times that of SCR technology for heavy duty application.

EGR systems are also used in diesel engines for lowering NO_X emissions. However with the use of EGR systems, the fuel economy decreases. This is because of incomplete combustion due to lower oxygen levels especially at higher loads. Compared to both EGR and LNT technologies, SCR has almost no impact on fuel economy while contributing to lowering emission levels at the same time. The use of urea SCR can bring down driving costs considerably. If LNT systems are replaced by SCR systems, the cost reduction can occur through the reduction in fuel consumption. According to the study conducted in [43], the overall lifetime cost difference between using SCR over LNT was calculated to be 7350 USD.

Although the study carried out Lambert *et al.* states SCR to be a cheaper aftertreatment solution compared to LNT and EGR, there are costs associated with using SCR technology in the form of AdBlue costs which is taken as a percentage of fuel cost. Although the carbon footprint associated with urea used for trucks is relatively small compared to the urea used for agriculture, it is worthy of being considered. We consider one of the tests carried out at the engine bench and calculate the fuel penalty and the increase in CO_2 footprint. The test is run for a WHTC cycle.

$$\text{Engine out } NO_X = 5.7 \text{ g/kWh} \tag{3.8}$$

A NO/NO_2 ratio of 63:37 in the NO_X after the DOC was calculated through measurements. The molar mass of NO_X is,

$$\text{Molar Mass of } NO_X = 46 \text{ g/mol} \tag{3.9}$$

Dividing 3.8 by 3.9 gives,

$$\text{Engine out } NO_X = 0.124 \text{ mol/kWh} \tag{3.10}$$

The overall ANR during the test was observed to be 1.09. Thus the consumption of NH_3 can be calculated by multiplying 3.10 with the ANR as shown below:

$$\text{Consumption of } NH_3 = 1.09.(\text{Engine out } NO_X \text{ [g/kWh]}) = 0.135 \text{ mol } NH_3\text{/kWh} \tag{3.11}$$

Since one mole of urea gives 2 moles of NH_3, the consumption of urea can be calculated as,

$$\text{Consumption of Urea} = \frac{\text{Consumption of } NH_3}{2} = 0.067 \text{ mol Urea/kWh} \tag{3.12}$$

The molar mass of Urea can be taken as 60 g/mol. Upon multiplying the molar mass of urea by the consumption of urea in moles we obtain,

$$\begin{aligned}\text{Urea consumption in g/kWh} &= (\text{Consumption of urea in mol/kWh}).(\text{Molar mass of urea}) \\ &= 4.05 \text{ g of urea/kWh}\end{aligned} \tag{3.13}$$

The concentration of urea in Adblue is 32.5 %. Thus the AdBlue consumption can be calculated to be

$$\text{AdBlue consumption} = \frac{\text{Urea consumption in g/kWh}}{0.325} = 12.46 \text{ g AdBlue/kWh} \tag{3.14}$$

Density of AdBlue at 20 °C is 1.08 kg/L. The price of AdBlue in Sweden is roughly half that of diesel. The price of diesel in Sweden is 13.55 SEK/L. Thus the price of Adblue is taken to be 6.7 SEK/L. Thus the cost per kWh of AdBlue can be calculated as,

$$\text{Cost per kWh of AdBlue} = \frac{(\text{AdBlue consumption}).(6.7)}{1.08.10^3} = 0.0844 \text{ SEK/kWh} \tag{3.15}$$

The efficiency for the engine used is assumed to be around 35 %. The BSFC of the engine can be calculated as,

$$\text{BSFC} = \frac{1}{\eta.LHV_{Diesel}} = 242 \text{ g/kWh} \tag{3.16}$$

The fuel cost per kWh is calculated as ,

$$\text{Fuel cost per kWh} = \frac{(\text{BSFC}).(\text{Fuel Cost})}{\text{Density of diesel}} = 4.15 \text{ SEK/kWh} \tag{3.17}$$

To calculate the AdBlue penalty as a percentage of the fuel consumed, we divide 3.15 by 3.17 which gives,

$$\text{AdBlue penalty} = \frac{\text{Cost per kWh of AdBlue}}{\text{Fuel cost per kWh}} = 2 \text{ \%} \tag{3.18}$$

The CO_2 footprint of AdBlue can now be calculated. One molecule of AdBlue releases one molecule of CO_2. Thus the contribution of CO_2 per kWh from the AdBlue is the same as the consumption of urea as calculated in 3.12.

The total CO_2 produced by the diesel fuel can be calculated by using the carbon content in diesel. The carbon content in diesel is 2.778 Kg/gallon or 0.73 Kg/L. The CO_2 produced per litre of diesel is calculated as,

$$CO_2 \text{ produced} = \frac{0.73.0.99.44}{12} = 2.649 \text{ kg of } CO_2\text{/l} \tag{3.19}$$

The CO_2 produced per gram of diesel is thus,

$$\begin{aligned} CO_2 \text{ produced from diesel per kWh} &= \frac{(2.649).(\text{BSFC})}{\text{Density of diesel}} \\ &= 811 \text{ g of } CO_2/\text{kWh} = 18.44 \text{ mol of } CO_2/\text{kWh} \end{aligned} \tag{3.20}$$

Thus the CO_2 penalty expressed as a percentage of total CO_2 emissions from diesel can be calculated as,

$$CO_2 \text{ penalty from AdBlue} = \frac{\text{AdBlue } CO_2 \text{ contribution}}{\text{Diesel } CO_2 \text{ contribution}} = 0.4 \text{ \% of total } CO_2 \text{ from diesel fuel.} \tag{3.21}$$

The total relative increase in the CO_2 footprint is calculated as using the CO_2 footprint per ton of NH_3 produced for western Europe from the previous section.

$$\begin{aligned} \text{Total relative } CO_2 \text{ footprint increase} &= (CO_2 \text{ penalty AdBlue}) + \\ &\quad (CO_2 \text{ penalty AdBlue}).(CO_2 \text{ footprint for western Europe}) \\ &= 1.22\% \end{aligned} \tag{3.22}$$

4

Numerical model of the SCR system

A model representing a state of the art extruded vanadia system was developed. The model is parameterized using engine test data. This chapter provides an overview of the structure of the model and the various chemical reactions modelled. The structure of the model is similar to the structure described in the previous chapter. The system is modelled based on the assumptions mentioned in section 2.2.1.

4.1 Overview of chemical kinetics modelled

A total of six chemical reactions have been modelled. The first two reactions modelled represent the adsorption and desorption of NH_3 on the surface of the catalyst. These reactions and their respective reaction rates are shown below:

$$NH_3 + S \longleftrightarrow NH_3{}^* \tag{4.1}$$

The reaction rates for adsorption are expressed as,

$$r_{ads} = k_{ads}.C_{NH3}.C_s.(1-\theta) \tag{4.2}$$

where θ is the surface coverage of the catalyst, C_s concentration of active surface atoms with respect to the gas volume in the converter, k_{ads} denotes the rate constant of the reaction and C_{NH3} denotes the gas phase concentration of ammonia.

The adsorption reaction is assumed to be a non-activated reaction and the ammonia is assumed to adsorb on the catalytic surface instantaneously.

The rate of desorption is expressed as,

$$r_{des} = k_{des}.e^{-(\frac{E_a}{R.T})}.C_s.\theta \tag{4.3}$$

where E_a denotes the activation energy for desorption, k_{des} denotes the rate constant for desorption and R denotes the universal gas constant.

After a brief literature review on the topic of NH_3 desorption from the surface of the SCR, the desorption was taken to be of Temkin-type [44] and the activation energy was taken to be a function of the surface coverage θ. The activation energy as a function of the surface coverage is expressed below,

$$E_a = \Delta H_{NH3}.(1-\alpha.\theta) \tag{4.4}$$

where ΔH_{NH3} denotes the constant of activation energy for desorption and alpha denotes the constant for surface coverage dependence. The next set of reactions modelled are the SCR reactions. These SCR reactions and their respective reaction rates are shown below:

$$4\,NH_3 + 4\,NO + O_2 \longrightarrow 4\,N_2 + 6\,H_2O \tag{4.5}$$

The rate of the standard SCR reaction is expressed as,

$$r_{std} = k_{std}.e^{-(\frac{E_{std}}{R.T})}.C_s.C_{NO}.\theta \tag{4.6}$$

where C_{NO} is the concentration of NO in the gas phase, E_{std} is the activation energy for the standard SCR reaction and k_{std} is the rate constant for the standard SCR reaction.

$$4\,NH_3 + 2\,NO + 2\,NO_2 \longrightarrow 4\,N_2 + 6\,H_2O \tag{4.7}$$

The rate of fast SCR reaction is expressed as,

$$R_{fast} = k_{fast}.e^{-(\frac{E_{fast}}{R.T})}.C_s.C_{NO}.C_{NO_2}\theta \tag{4.8}$$

where E_{fast} is the activation energy for the fast SCR reaction and k_{fast} is the rate constant for the fast SCR reaction.

Initially the slow SCR reaction was not modelled. However upon running further tests on the extruded vanadia catalyst, it was observed that the slow SCR reaction occurred around the operating temperatures of the catalyst. Thus the slow SCR reaction was included in the model.

$$8\,NH_3 + 6\,NO_2 \longrightarrow 7\,N_2 + 12\,H_2O \tag{4.9}$$

$$r_{slow} = k_{slow}.e^{-(\frac{E_{slow}}{R.T})}.C_s.C_{NO_2}\theta \tag{4.10}$$

The last set of reactions modelled are the oxidation reactions which describe the oxidation of NH_3 on the catalyst surface. Since diesel combustion is a lean combustion there is always excess of oxygen, hence the oxidation reaction is assumed to be independent of oxygen concentration.

$$4\,NH_3 + 3\,O_2 \longrightarrow 2\,N_2 + 6\,H_2O \tag{4.11}$$

$$r_{ox} = k_{ox}.e^{-(\frac{E_{Ox}}{R.T})}.C_s.\theta \tag{4.12}$$

These reaction rates are then used to calculate the surface coverage of the SCR catalyst as a function of time. This can be expressed by the following equation:

$$\dot{\theta} = r_{ads} - r_{des} - 2.r_{fast} - 4.r_{slow} - r_{std} - 2.r_{ox} \tag{4.13}$$

The rates are also used to calculate the individual concentrations of NO, NO_2 and NH_3. The individual concentrations can be calculated as,

$$C_{NH3} = \frac{(\frac{N_{Cell}}{\epsilon.V_c}).\dot{n}_{NH_3,in} + r_{des}}{(\frac{R_{ex,gas}}{P_{amb}}).(\frac{N_{Cell}}{\epsilon.V_c}).\dot{m}_{exgas}.T + k_{ads}.C_s.(1-\theta)} \tag{4.14}$$

$$\dot{C}_{NO} = (\frac{N_{Cell}}{\epsilon.V_c}).\dot{n}_{NO,in} - (\frac{N_{Cell}}{\epsilon.V_c}).\dot{n}_{NO,out} - r_{fast} - r_{std} \tag{4.15}$$

$$\dot{C}_{NO2} = (\frac{N_{Cell}}{\epsilon.V_c}).\dot{n}_{NO_2,in} - (\frac{N_{Cell}}{\epsilon.V_c}).\dot{n}_{NO_2,out} - r_{fast} - r_{slow} \tag{4.16}$$

Consider equation 4.14. The concentration of NH_3 is in [mol/m^3] and the units of $\dot{n}_{\mathrm{NH_3},in}$ is in [mol/s]. Upon cross-multiplying the denominator of 4.14 with the LHS of the equation and rearranging the terms equation 4.14 can be expressed as,

$$\dot{n}_{NH3,out}.N_{cell} = \dot{n}_{NH3,in}.N_{cell} + r_{des} - r_{ads} \tag{4.17}$$

All the terms in equation 4.17 have the units [mol/m^3 s].

For a 3-cell model, the concentration of NH_3, NO and NO_2 calculated in the first cell is carried forward to the second cell where the SCR reactions occur again. The concentrations of NH_3, NO and NO_2 from the second cell is carried forward to the third cell.

Equations 4.14-4.16 show how the concentrations are calculated in an SCR Cell. For a 3-cell model these equations would give the concentrations of NH_3, NO and NO_2 in the first cell. The concentrations in the second cell can be calculated as shown below:

$$C_{NH3,2} = \frac{(\frac{N_{Cell}}{\epsilon.V_c}).\dot{n}_{\mathrm{NH_3},cell1out} + r_{des,cell2}}{(\frac{R_{ex,gas}}{P_{amb}}).(\frac{N_{Cell}}{\epsilon.V_c}).\dot{m}_{exgas}.T_{cell2} + k_{ads}.C_s.(1-\theta)} \tag{4.18}$$

$$\dot{C}_{NO,2} = (\frac{N_{Cell}}{\epsilon.V_c}).\dot{n}_{\mathrm{NO},cell1out} - (\frac{N_{Cell}}{\epsilon.V_c}).\dot{n}_{\mathrm{NO},cell2out} - r_{fast} - r_{std} \tag{4.19}$$

$$\dot{C}_{NO2,2} = (\frac{N_{Cell}}{\epsilon.V_c}).\dot{n}_{\mathrm{NO_2},cell1out} - (\frac{N_{Cell}}{\epsilon.V_c}).\dot{n}_{\mathrm{NO_2},cell2out} - r_{fast} - r_{slow} \tag{4.20}$$

4.1.1 Scaling of storage capacity

The storage capacity which is denoted by C_s is a variable that is automatically scaled with the volume of the catalyst. The units of the storage capacity C_s is expressed in [mol/m^3]. The scaling of the storage capacity of the catalyst is explained with an example to ensure better understanding. Let us consider the calculation of the concentration of NH_3 (g) inside the catalyst. It is expressed as shown by equation 4.14. Upon cross multiplying the denominator, equation 4.14 can be expressed as,

$$C_{NH3}.(\frac{R_{ex,gas}}{P_{amb}}).(\frac{N_{Cell}}{\epsilon.V_c}).\dot{m}_{exgas}.T) + C_{NH3}.k_{ads}.C_s.(1-\theta) = (\frac{N_{Cell}}{\epsilon.V_c}).\dot{n}_{\mathrm{NH_3},in} + r_{des} \tag{4.21}$$

Upon using the ideal gas law and the rate equation for desorption, equation 4.21 can be expressed as,

$$\dot{n}_{NH3,out}.\frac{N_{Cell}}{\epsilon.V_c} = \dot{n}_{NH3,in}.\frac{N_{Cell}}{\epsilon.V_c} + k_{des}.e^{-(\frac{E_a}{R.T})}.C_s.\theta - C_{NH3}.k_{ads}.C_s.(1-\theta) \tag{4.22}$$

where V_c is the volume of the catalyst. Upon multiplying both sides of equation (4.22) by $\epsilon.V_c$ we get

$$\dot{n}_{NH3,out}.N_{cell} = \dot{n}_{NH3,in}.N_{cell} + k_{des}.e^{-(\frac{E_a}{R.T})}.C_s.\theta.\epsilon.V_c - C_{NH3}.k_{ads}.C_s.(1-\theta).\epsilon.V_c \tag{4.23}$$

The term $\epsilon.V_c$ gives the gas volume or open volume of the catalyst in m_3. Thus, upon multiplying this term by C_s which is expressed per m^3 of catalyst volume, the NH_3 storage capacity of the catalyst for any particular volume of the catalyst is obtained.

4.2 Temperature Model

The temperature model is a simplified model. The heat losses to the surroundings are assumed to be minimal as the SCR is well insulated. Therefore radiative and convective losses to the environment are neglected. The temperature model can be expressed through the following equation,

$$\dot{T}_{SCR} = \frac{N_{Cell,T}.C_{p,exgas}.\dot{m}_{exgas}.(T_{exgas} - T_{SCR})}{C_{p,SCR}.m_{SCR}}. \tag{4.24}$$

The effect of radiation was tested by adding an additional equation for the radiation loss. However, the heat losses due to radiation were observed to be minimal and the term was removed from the model.

Initially the temperature model comprised of 3 cells. When the temperature model was tested with test data, it was observed that although the temperature model captured the dynamics of the real system, there was still more room for improvement.

Upon extending the number of cells to 9, the temperature profile of the SCR captured the dynamics of the real SCR system better. This is shown in figure 4.1.

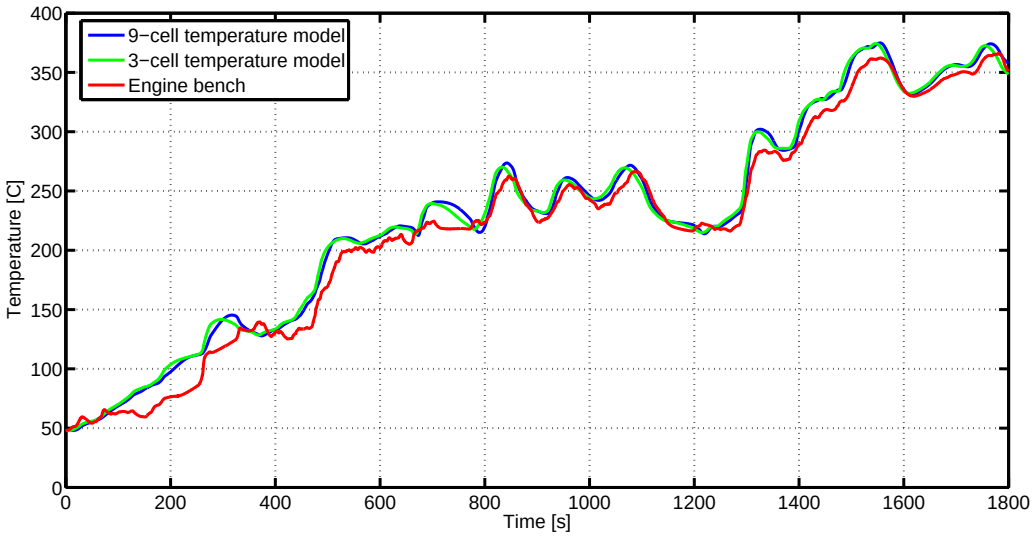

Figure 4.1: 3 cell Temperature model vs 9 cell temperature model

The temperature model was extended by discretizing the SCR system into 9 cells.

The SCR system is discretized into 3 cells to capture the reaction kinetics and each of these cells comprises of 3 cells of the temperature model. Figure 3.1 represents the discretization carried out on the SCR system:

After an additional but brief literature review, the specific heat capacities of the exhaust gas as well as the SCR monolith were considered to be functions of temperature. The key point to be noted is that, the model is intended to be simple yet capture the dynamics of the real system. More accurate temperature models of SCR systems are available as mentioned in the previous chapter and can be utilised for future use.

The modified specific heat of exhaust gas as a function of temperature can be expressed as,

$$C_{p,exgas} = A_1 - \frac{A_2}{T_{exgas}^2} + A_3.T_{exgas} + A_4.T_{exgas}^2 \tag{4.25}$$

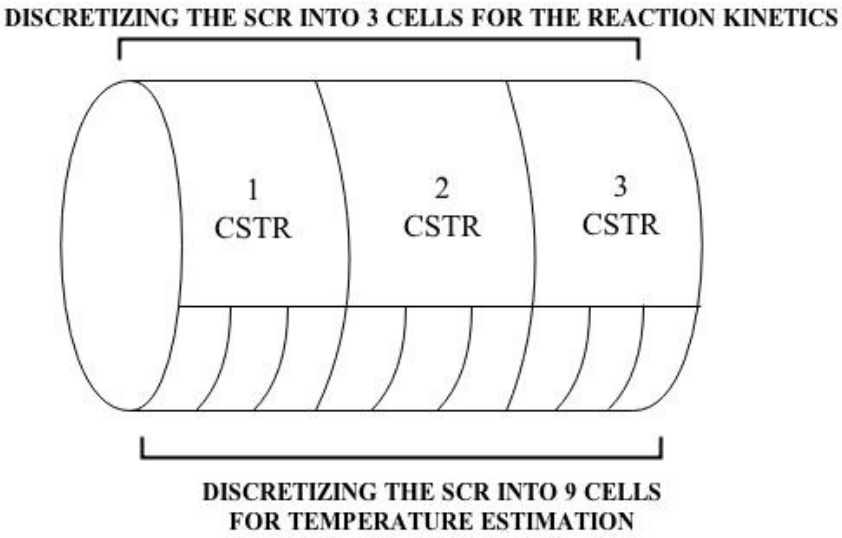

Figure 4.2: Discretization of the SCR into 3 CSTRs for the reaction kinetics and 9 cells for temperature estimation

where A_1, A_2, A_3 and A_4 are constants specific to exhaust gas. These constants were taken from the JM model.

The modified specific heat of the substrate as a function of temperature can be expressed as,

$$C_{p,substrate} = M_1 + M_2.T_{SCR} - M_3.T_{SCR}.^2 \tag{4.26}$$

where M_1, M_2 and M_3 are constants specific to the substrate material. These constants were taken from the JM model.

4.2.1 Heat losses through the exhaust pipe and urea decomposition

Engine bench data for the WHTC and WHSC cycles were obtained for the purpose of tuning the parameters of the system to engine bench data. However it was observed that the temperature measured at the inlet of the SCR was inaccurate due to the wetting of the temperature sensor with droplets of AdBlue solution. In order to obtain a fairly good estimate of the temperature of the inlet of the SCR, heat losses due to urea decomposition and through the exhaust pipe were modelled. The description of the model is provided in this section.

Due to the high temperature of the exhaust gas, AdBlue injected upstream of the SCR decomposes into urea which gets then reduced to ammonia and iso-cyanic acid. Water evaporates first which causes a decrease in the temperature of the exhaust gas. This is because evaporation of water is a cooling process which utilizes the heat from the exhaust gas lowering the temperature of the exhaust gas. The model representing the heat losses due to urea decomposition can be shown by the following expression:

$$\begin{aligned} Q_{AdB} = [&(L_{v,\mathrm{H_2O}} + (T_{b,\mathrm{H_2O}} - T_{amb}).C_{p,\mathrm{H_2O}(l)} + (T_{out} - T_{b,\mathrm{H_2O}}).C_{p,\mathrm{H_2O}(g)}).(1-\gamma) \\ &+ (T_{out} - T_{amb}).C_{p,Urea}.\gamma].\dot{m}_{urea} \end{aligned} \tag{4.27}$$

Equation 4.27 represents the heat absorbed by AdBlue to decompose into urea.
The heat lost by the exhaust gas can be expressed by,

$$Q_{exgas} = C_{p,exgas}.\dot{m}_{exgas,US}.T_{in} - C_{p,exgas}.(\dot{m}_{exgas,US} + \dot{m}_{urea}).T_{out} \tag{4.28}$$

Solving for T_{out} and rearranging the terms we arrive at the following equation,

$$T_{out} = \frac{\begin{array}{c} C_{p,exgas}.\dot{m}_{exgas,US}.T_{in} + \dot{m}_{urea}.[(1-\gamma).C_{p,\mathrm{H_2O}(g)}.T_{b,\mathrm{H_2O}} + T_{amb}.C_{p,Urea}.\gamma \\ -(T_{b,\mathrm{H_2O}} - T_{amb}).C_{p,\mathrm{H_2O}(l)} - L_{v,\mathrm{H_2O}}.(1-\gamma)] \end{array}}{C_{p,exgas}.(\dot{m}_{exgas,US} + \dot{m}_{urea}) + \dot{m}_{urea}.C_{p,Urea}.\gamma + C_{p,\mathrm{H_2O}(g)}.(1-\gamma)} \tag{4.29}$$

In addition to the heat losses due to urea decomposition, there are heat losses through the exhaust pipe. The model used has been adopted from [45] proposed by Lars Erikson. The model of the exhaust pipe is a mean-value model. Figure 4.3 represents the heat losses through the exhaust pipe upstream of the catalyst.

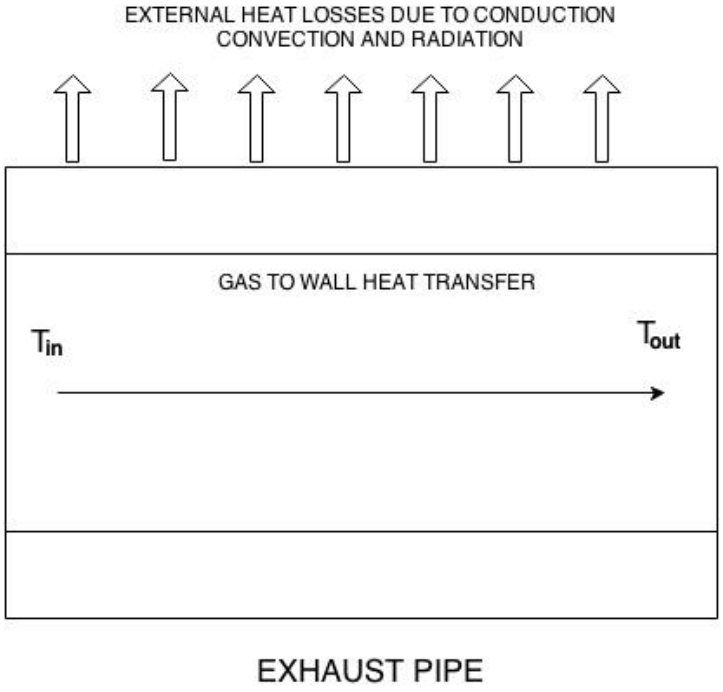

Figure 4.3: Heat losses through the exhaust pipe

The heat losses in the exhaust pipe can be split into internal heat losses and external heat losses. The internal heat losses involve heat losses from the exhaust gas to the pipe wall while the external involve convective and radiative heat losses to the surroundings. Calculating the internal and external heat losses, the wall temperature can be calculated.

$$\dot{Q}_{external} = A.[h_{cv,ext}.(T_{wall} - T_{amb}) + \sigma_{SB}.F_v.\epsilon_{rad}.(T_{wall}^4 - T_{amb}^4)] \tag{4.30}$$

$$\dot{Q}_{internal} = [h_i.A.(T_{exgas} - T_{wall})] \tag{4.31}$$

$$\frac{dT_{wall}}{dt} = \dot{Q}_{internal} - \dot{Q}_{external} \tag{4.32}$$

In the expression 4.30, the radiation term can be factored into

$$Q_{radiation} = A.[\sigma_{SB}.F_v.\epsilon_{rad}.(T_{wall}^2 + T_{amb}^2).(T_{wall} + T_{amb}).(T_{wall} - T_{amb})] \tag{4.33}$$

Equation 4.33 can be rewritten as

$$Q_{radiation} = h_{rad}.(T_{wall} - T_{amb}) \tag{4.34}$$

where h_{rad} is a lumped non-linear term. This is done mainly because this transforms the radiation expression into a form similar to the convective equation. The term h_{rad} can be used to compare the respective heat transfer coefficients.

The wall temperature calculated from equation (4.32) can be used to calculate the temperature of the exhaust gas at the outlet of the exhaust pipe.

The expression for the temperature drop in the can be determined through the means of a partial differential equation. To determine the expression for the temperature drop in the pipe, a small slice of the pipe is considered with a length of dx. The pipe is assumed to be straight for simplicity. A schematic diagram of the pipe is shown below:

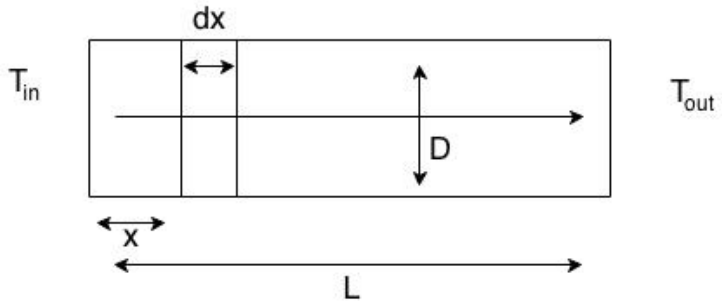

Figure 4.4: Schematic diagram of the pipe considered for the derivation

The small section of the pipe is considered at a distance (x+$\frac{dx}{2}$) from the inlet of the pipe. As the exhaust gas passes through the pipe, the temperature of the gas decreases along the length of the pipe. The temperature at the end of the small section is considered to be T_s. The surface area of the small section can be given by

$$A_s = \pi.dx.D \tag{4.35}$$

Thus the heat flux through this small section can be given by

$$\dot{Q} = A_s.h_s.(T_s - T_{wall}) \tag{4.36}$$

Writing the expression for the heat lost by the exhaust gas from the beginning of the section at a distance (x-$\frac{dx}{2}$) to the end of the section at (x+$\frac{dx}{2}$)

$$\dot{Q} = \dot{m}_{exgas}.C_{p,exgas}.(T_{x+\frac{dx}{2}} - T_{x-\frac{dx}{2}}) \tag{4.37}$$

Setting (4.36) equal to and taking the limit as dx $\rightarrow$ 0, the following PDE is obtained

$$\frac{-dT_{wall}}{dx} = \frac{h_s.\pi.D.(T_s - T_{wall})}{\dot{m}_{exgas}.C_{p,exgas}} \tag{4.38}$$

Solving the above equation through the method of separation of variables the final expression for the outlet temperature of the pipe is obtained

$$T_{pipe,out} = T_{wall} + (T_{exgas} - T_{wall}).e^{-\frac{h_{cv,i}.A_{pipe}}{\dot{m}_{exgas}.C_{p,exgas}}} \tag{4.39}$$

The pipe model along with the model for urea decomposition is coupled with the SCR model and is used to obtain a estimate of the SCR temperature. During the tests with the model, it was

observed that the temperature drop in the exhaust gas due to the decomposition of AdBlue is not significant. Hence the model for temperature loss due to urea composition was not was not used during the simulation. However the pipe model was retained as there were significant heat losses from the exhaust pipe. Figure 4.5 shows the SCR out gas temperature after including the pipe model.

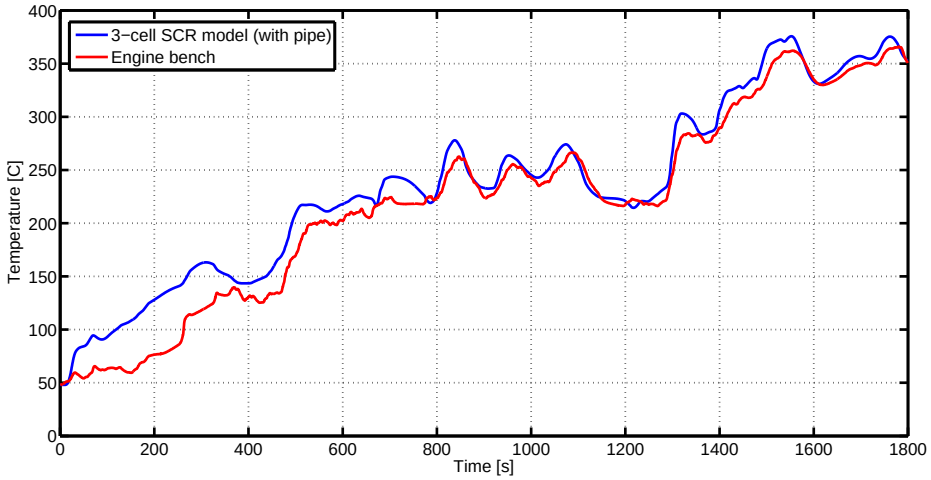

Figure 4.5: SCR temperature with the pipe model

From figure 4.5 it can be seen that a good estimate of the temperature at the inlet of the SCR is obtained. The following table lists the heat transfer coefficients used in the model:

Table 4.1: Heat transfer coefficients

Parameter	**W/ K** m^2
$h_{external}$	30
$h_{internal}$	400
$h_{convection}$	80
$h_{radiation}$	30

From the measurements of the SCR temperature for a WHTC test cycle, it was observed that the average drop in temperature of the exhaust gas was around 27 °C from the outlet of the DOC till the inlet of the SCR. To check the performance of the pipe model, 27 °C was subtracted from the temperature measured after the DOC which was then given in the feed to the SCR model to obtain an estimate of the SCR temperature. Figure 4.6 shows the comparison for the SCR temperature obtained with the pipe model and by subtracting 27 °C from the exhaust gas temperature.

From the above figure, it might seem that subtracting 27 °C might be a better option. However the curve for this case agrees well only in the beginning of the cycle while the temperature obtained with the pipe model shows a higher temperature. This is mainly because during the beginning of cycle the drop in temperature is well below 27 °C and this value is the average value for the entire cycle. Thus, it is a better idea to run the SCR model with the exhaust pipe model as well as the model for urea decomposition. The temperature of the SCR model seems to deviate from that of the engine bench during the first 300 seconds. One of the reasons for this could be that the initial temperature of the exhaust pipe is wrong. The initial temperature of the exhaust pipe was assumed as a true measure of the initial temperature of the pipe was not available.

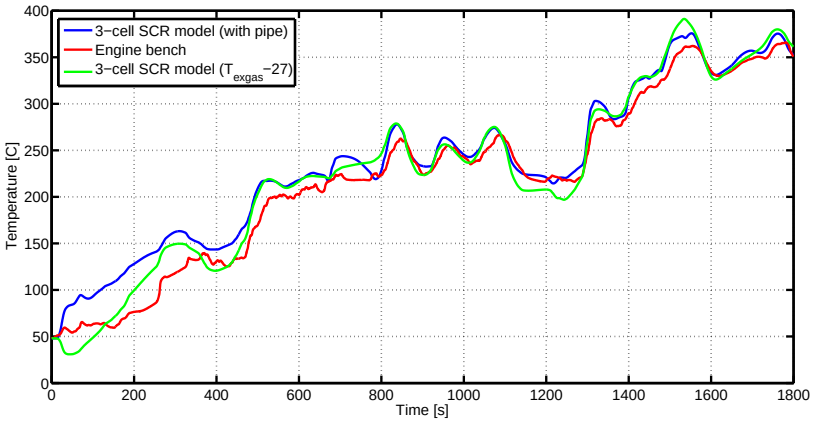

Figure 4.6: SCR temperature with the pipe model and without the pipe model

4.3 Parameter Estimation

The previous section mentioned the modeling part of the SCR kinetics. This section will explain the process of parameter identification for the SCR kinetics. A total of 13 parameters had to be identified. An existing detailed kinetic model of the SCR developed by Johnson Matthey was available. This detailed kinetic model served as a virtual gas bench to conduct the various tests to identify the parameters. This leads to a quicker lead time and flexibility in conducting the tests. Flexibility here refers to the ease of changing the gas composition.

The parameters to be identified are the pre-exponential factor for the 6 reactions and the activation energy for 5 reactions. The adsorption is assumed to be a non-activated reaction hence the activation energy of adsorption is 0. Two other parameters that were estimated are 'alpha' that takes into account the variation in the activation energy as a function of number of filled sites and 'C_s' which is the NH_3 storage capacity of the catalyst. The term C_s is the capacity equivalence in the gas phase to the surface capacity. C_s does not have a physical meaning as capacity is a surface phnomenon.

The parameters in the detailed kinetic model of Johnson Matthey were for an aged catalyst. In order to validate the model for a fresh catalyst the parameters of the 3 cell model were calibrated to the engine bench data from a fresh catalyst.

A 3 cell SCR and a 5 cell SCR were modeled. It was observed that there were no significant differences between a 3 and 5 cell model, therefore the 3 cell model was retained. The 3 cell model has a prediction of NO_X and NH_3 out for both the steady and transient response. Moreover a 3 cell model would be computationally less demanding than a 5 cell and is faster, which would render it better for control purpose.

To accomplish this task, the MATLAB® function *fminsearchbnd* was used [46]. The cost function formulated is shown in equation 4.40.

$$J = \Sigma[\frac{(\mathrm{NO}_{2meas} - \mathrm{NO}_{2sim})^2}{var(\mathrm{NO}_{2meas} - \mathrm{NO}_{2sim})} + \frac{(\mathrm{NH}_{3meas} - \mathrm{NH}_{3sim})^2}{var(\mathrm{NH}_{3meas} - \mathrm{NH}_{3sim})} + \frac{(\mathrm{NO}_{meas} - \mathrm{NO}_{sim})^2}{var(\mathrm{NO}_{meas} - \mathrm{NO}_{sim})}] \quad (4.40)$$

The cost function is divided by variance to give equal importance to all the 3 terms in equation 4.40. Otherwise fminsearch has an inclination to reduce the term that has a greater influence on the cost function.

4.3.1 Steps involved in parameter estimation

1. Identification of the kinetic parameters for adsorption, desorption and capacity:

   This is the first step in the parameter identification process. The input feed containing 1500 ppm of NH_3 is turned on at 1000 seconds while the temperature of SCR is maintained at a constant temperature of 150 °C. The mass flow rate is at 0.5 kg/s throughout this test. 1500 ppm of ammonia is fed for approximately 1600 seconds and then turned off. After a while the temperature is raised linearly at 15 °C per minute till 450 °C. This process ensures that all the ammonia adsorbed on the catalyst desorbs completely by increasing the temperature. This step is called TPD (Temperature programmed desorption), this is carried out to determine the capacity of the catalyst that is the total ammonia adsorption capacity in moles.

   By carrying out TPD 5 kinetic parameters are identified using an optimization routine with fminsearch in Matlab. The parameters identified are : 1. k_{ads} - pre exponential factor for adsorption 2. k_{des} - pre exponential factor for desorption 3. Ea_{des} - Activation energy for desorption 4. α - Constant which ensures that activation energy for desorption is a function of surface coverage (θ) 5. C_s - Capacity in gas phase.

   Figure 4.7 shows the comparison between the 3 cell model and the detailed kinetic model once the parameters are estimated using fminsearch. There is a good agreement between both the models.

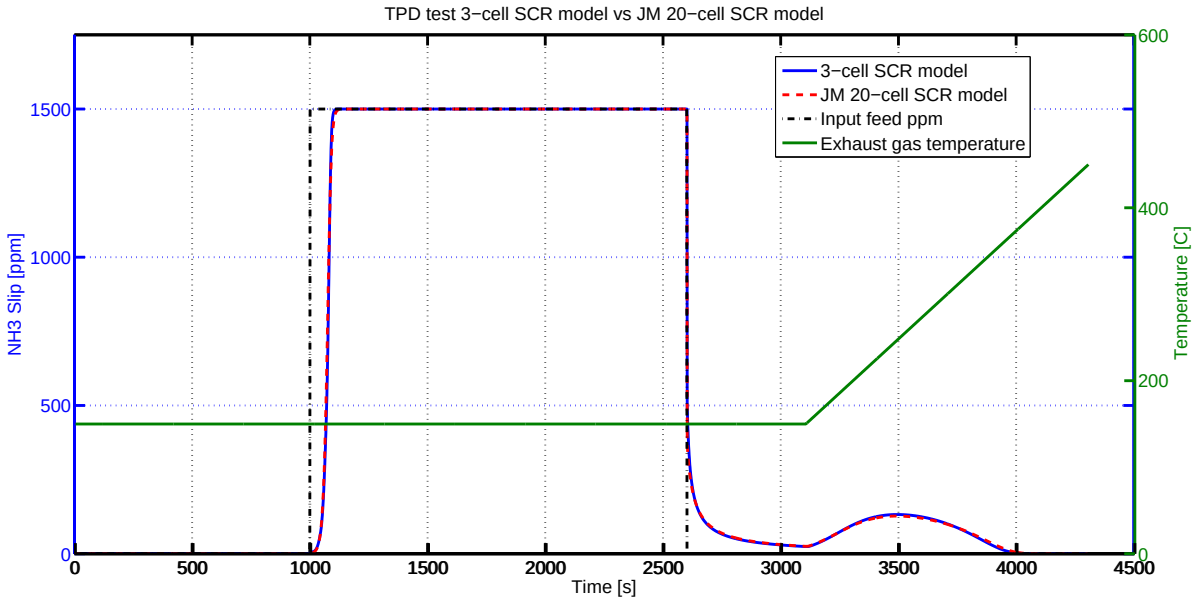

Figure 4.7: TPD test comparison of JM model vs 3 cell model

2. Identification of the kinetic parameters for standard SCR reaction:

   The second step in the parameter identification involves identifying the rate constant for the standard SCR reaction. As mentioned earlier the SCR reaction involves reaction with only NO. The feed which contains the mass flow rate of exhaust gas, NH_3 and NO is varied in steps and turned on/off as shown in figure 4.8 and 4.9. Two parameters are estimated which is the pre exponential constant and the activation energy for standard SCR.

Once the optimization is complete and parameters identified there is a good agreement between the 3 cell and the JM model. This agreement can be seen in figure 4.8 and 4.9.

3. Identification of the kinetic parameters for slow SCR reaction:

   Once the kinetic parameters for the standard SCR have been identified the next step is to identify the parameters related to the standard SCR. In this step the input feed consists of only NO_2 gas and NH_3. An optimization routine as mentioned earlier is carried to identify the parameters. The parameters estimated in this step are the pre exponential factor and activation energy for slow SCR.

4. Identification of the kinetic parameters for fast SCR reaction:

   The fast SCR reaction is one of the most important reactions in an SCR as this it the fastest reaction. The rate constant for the fast SCR is one order of magnitude higher than the standard SCR. To identify the rate constants for the fast SCR the input feed gas has equal proportion of NO and NO_2. The ANR, mass flow rate and temperature are varied in steps. Once again the optimization routine is run with fminsearch to identify the two parameters which are the pre exponential factor and the activation energy of fast SCR.

5. Identification of the kinetic parameters for NH_3 oxidation reaction:

   Once all the parameters related to the SCR reactions have been identified the final step is to identify parameters for NH_3 oxidation reaction. In this process 10 % oxygen is included in the feed. In all the previous reaction oxygen was not present in the feed. This is carried out to identify the parameters for the rate constant for oxidation of ammonia to nitrogen.

   Once all parameters are identified step wise. In figure 4.8 and 4.9 it can be seen there is a good agreement in the transient and steady state behavior of the two models. There is a slight discrepancy in the steady state values and this can be attributed to the following:
   1. Number cells 2. JM model is a detailed kinetic model which has more reactions and includes mass transfer effects which the 3 cell model ignores.

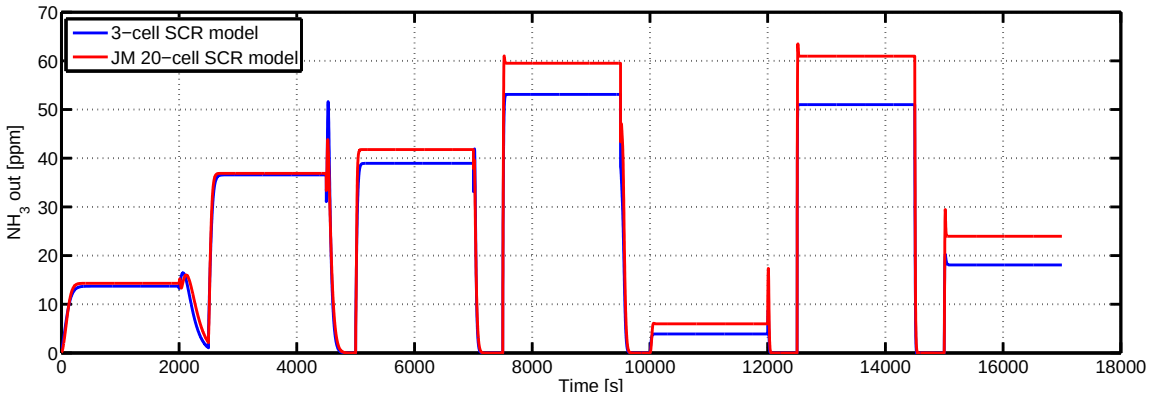

Figure 4.8: Ammonia slip comparison for a 3 cell and the detailed kinetic model with all parameters estimated

Table 4.2 gives the estimated values for the parameters after the parameter identification procedure. The initial guesses are also shown.

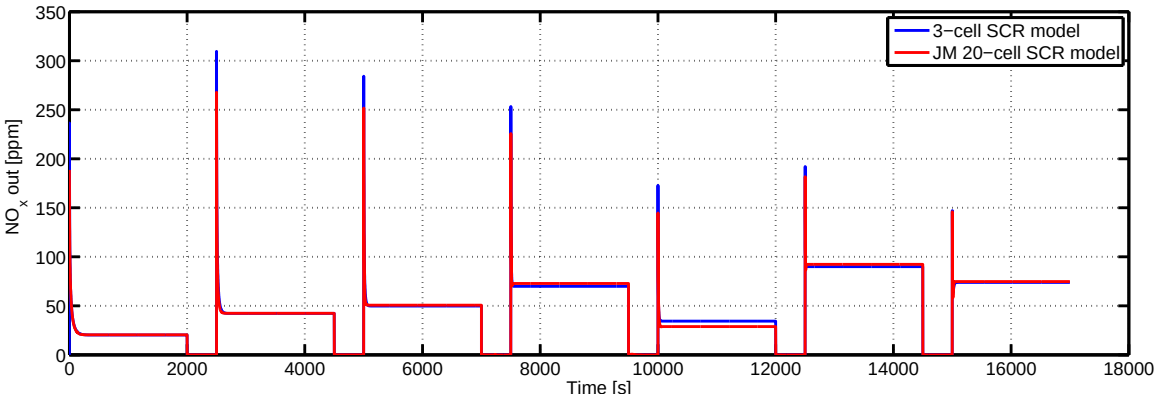

Figure 4.9: NO_X out comparison for a 3 cell and the detailed kinetic model with all parameters estimated

Table 4.2: Estimated parameters for SCR kinetics

Parameter	Symbol	Value	Initial guess	Lower bound	Upper bound
Pre exponential factor adsorbtion	k_{ads}	5.796	5	0	+inf
Pre exponential factor desorbtion	k_{des}	1.09e6	6e5	0	+inf
Activation energy desorbtion	Ea_{des}	81.7e3	81e4	25e3	250e3
Alpha	α	0.1871	0.2	0	1
Capacity	C_s	146.21	150	75	250
Pre exponential factor fast scr	$k_{fastSCR}$	4.18e11	5e11	0	+inf
Activation energy fast scr	$Ea_{fastSCR}$	6.85e4	67e3	25e3	250e3
Pre exponential factor standard scr	k_{stdSCR}	1.56e7	2.74e8	0	+inf
Activation energy standard scr	Ea_{stdSCR}	6.37e4	75e3	25e3	250e3
Pre exponential factor slow scr	$k_{slowSCR}$	2.28e10	5e10	0	+inf
Activation energy slow scr	$Ea_{slowSCR}$	1.06e5	1e5	25e3	250e3
Pre exponential factor oxidation	k_{ox}	1.18e12	2.4e9	0	+inf
Activation energy oxidation	Ea_{ox}	1.81e5	40e3	25e3	250e3

4.3.2 Sensitivity analysis

This section gives an overview of the sensitivity analysis carried out on the SCR model to understand how variations in estimated parameters affect the output of the model. Sensitivity analysis is a study of how variations in the output of a model can be linked to variations in the inputs to the model. Changes in parameters have a direct influence on the states of the system. This in turn has a direct influence on the output from the model. Variations in the output of the model has a direct influence on the cost function used for optimizing the parameters.

Through a sensitivity analysis, the parameters can be ranked depending on the order of influence and the parameters with the most significant influence on the cost function can be tuned. A sensitivity analysis also helps in defining an effective cost function for parameter estimation. The cost function used for parameter estimation has already been shown in the previous section on parameter estimation.

Each parameter is changed by a small amount one at a time and the influence of this change is observed on the output of NO, NO_2 and NH_3 concentrations respectively. The overall sensitivity of the cost function is also observed. Each parameter is varied by ± 1 %. A sensitivity index is used to quantify the influence of each of the parameters. The sensitivity index can be defined as,

$$S_{Param} = \frac{(J_{varied} - J_{optimal}).P_{optimal}}{(P_{varied} - P_{optimal}).J_{optimal}} \tag{4.41}$$

where J_{varied} is the value that the cost function takes when upon varying the parameter [47] and P_{varied} is the varied value of the parameter from the optimal value. The parameters are varied in steps of 0.5 %.

The following table gives the sensitivity indices for the parameters estimated:

Table 4.3: Sensitivity indices for the parameters estimated

Parameter	S_{param} **-1**%	S_{param} **-0.5**%	S_{param} **+0.5**%	S_{param} **+1**%
$k_{fastSCR}$	0.007	0.004	0.005	0.004
$Ea_{fastSCR}$	0.087	0.086	0.086	0.095
k_{des}	0.010	0.03	0.008	0.007
$\Delta H_{\mathrm{NH_3}}$	0.108	0.121	0.148	0.159
k_{stdSCR}	0.027	0.027	0.023	0.022
Ea_{stdSCR}	0.380	0.379	0.355	0.350
k_{ads}	0.011	0.003	0.008	0.007
$k_{slowSCR}$	0.005	0.001	0.007	0.011
$Ea_{slowSCR}$	0.260	0.268	0.293	0.310
k_{ox}	0.001	0.002	0.010	0.004
Ea_{ox}	0.129	0.121	0.100	0.088
C_s	0.019	0.015	0.011	0.018
alpha	0.008	0.002	0.003	0.003

From the table, it can be observed that the cost function is influenced most by the activation energy for the standard SCR reaction followed by the activation energy for the slow SCR reaction. The activation energy of the oxidation of NH_3 also seems to have a rather significant influence on the cost function value. The following plots show the variation of the cost function with the variation of the parameter. The variation is shown as a relative variation of the parameters with respect to the optimal value while the variation in the cost function is shown relative to the value of the cost function at the optimal value.

$$J_{Relative} = \frac{J_{variedparam}}{J_{optimalparam}} \tag{4.42}$$

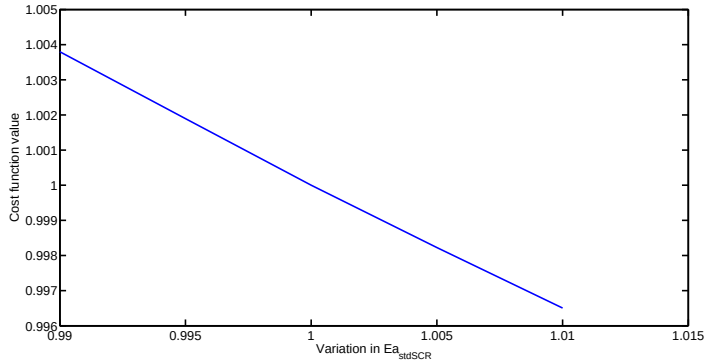

Figure 4.10: Variation in the relative cost function with variation in Ea_{stdSCR}

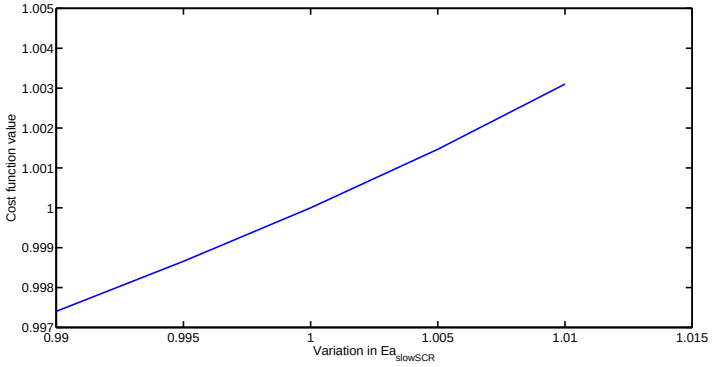

Figure 4.11: Variation in the relative cost function with variation in Ea_{slow}

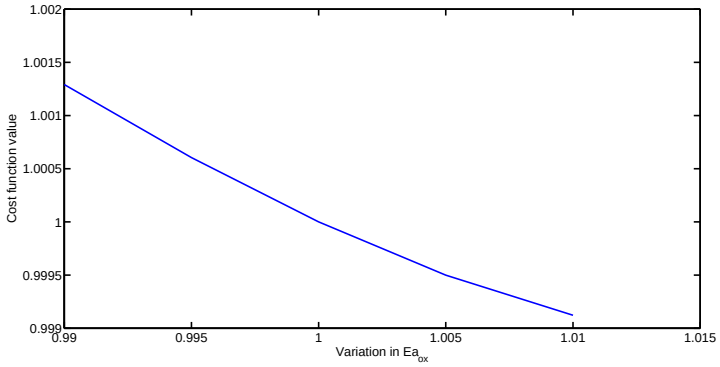

Figure 4.12: Variation in the relative cost function with variation in Ea_{ox}

From the sensitivity analysis one can see the three parameters which can be further tuned. This analysis can also be used to determine the minimum number of parameters which can be tuned. Although we perform a sensitivity analysis, the tuning of the parameters is not performed as a part of this thesis and has been left for future applications.

Computational time

The 3-cell model was extended to 20-cells and the time required to run the model was calculated through MATLAB using the profiler option. The JM 20-cell SCR model was then run in MATLAB and the time required to run that was also calculated using the profiler. The JM kinetic model was then reduced to just 3-cells and the time required to run was checked. Both the models were given CSF out emissions for three consecutive WHTC cycles as the feed.

After one cycle the engine is stopped for a period of ten minutes before the next cycle is started. To account for this, the temperature of the SCR in the model was reset to the temperature of the real SCR system just before the second cycle was started. As already mentioned in earlier sections, a single WHTC cycle is run for a period of 1800 s. The total run time for the three cycles is thus 5400 s. Table 4.4 gives the time required to run all the 4 cases. The simulations were run on a laptop equipped with 8 gigabytes of DDR3 RAM and an i7 Intel processor with a clockspeed of 2.3 GHz and 4 cores.

Table 4.4: Computational time required to run both the models

Model	Cells	Total time [s]	Simulation time/ real time second
JM	20	1797.298	0.33
Mean value SCR model	20	47.724	0.00883
JM	3	489.6	0.0906
Mean value SCR model	3	6.216	0.00115

From the above table it can be seen that although the 3-cell SCR model was extended to 20-cells, the time required to run is still significantly shorter compared to the detailed kinetic model provided by JM. The model takes lesser time to run while capturing most of the dynamics of the real SCR system which was one of the goals behind building the model. The model was built keeping in mind applicability for control applications. In modern ECUs, the calculations are done in real-time and thus the model of the SCR system needs to be quick in performing calculations.

Figure 4.13 shows a comparison between the JM 20-cell model, mean-value 20 cell model and engine bench.

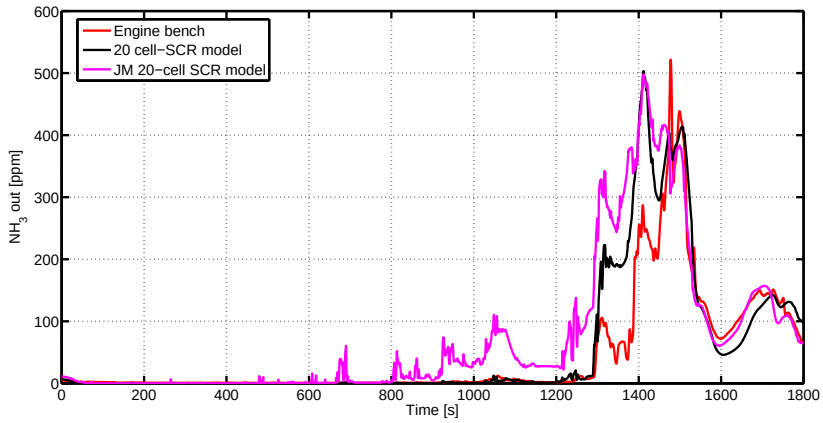

Figure 4.13: JM 20 cell SCR model vs mean-value 20 cell model

From figure 4.13 shown above, it can be seen that although the 20 cell model was run with parameters estimated for a 3-cell model, it still shows better agreement with the engine bench compared to the JM 20 cell model. As mentioned in an earlier section, the JM 20 cell model is a very detailed kinetic model which takes into account most of the reactions that can occur in an SCR system along with various mass transfer relations. Despite the complexity of the JM 20 cell model it does not capture the behaviour of the real SCR system compared to the mean-value 20 cell model. It can be said with certainty that with a good set of parameters, the mean-value 20 cell model can correlate even better with the real SCR system. Thus in this case, the complexity of the model plays no role in determining the agreement with the real system. However, a more complex model will definitely help analyze the presence of other chemical species which are of interest, primarily N_2O produced as a by-product of other side reactions.

4.4 Model validation

Once a set of parameters were obtained, the SCR model was validated with different sets of engine bench data for the WHTC cycle. The figure 4.14 and 4.15 shows the goodness of fit between the three cell SCR model and the engine bench data for flat ANR dosing of 1.2 for the WHTC cycle with a catalyst volume of 7.1 litres. Figure 4.14 shows the comparison of SCR out NO_X for the engine bench and the 3 cell SCR model. Figure 4.15 shows the comparison of SCR out NH_3 for the engine bench and the 3 cell SCR model.

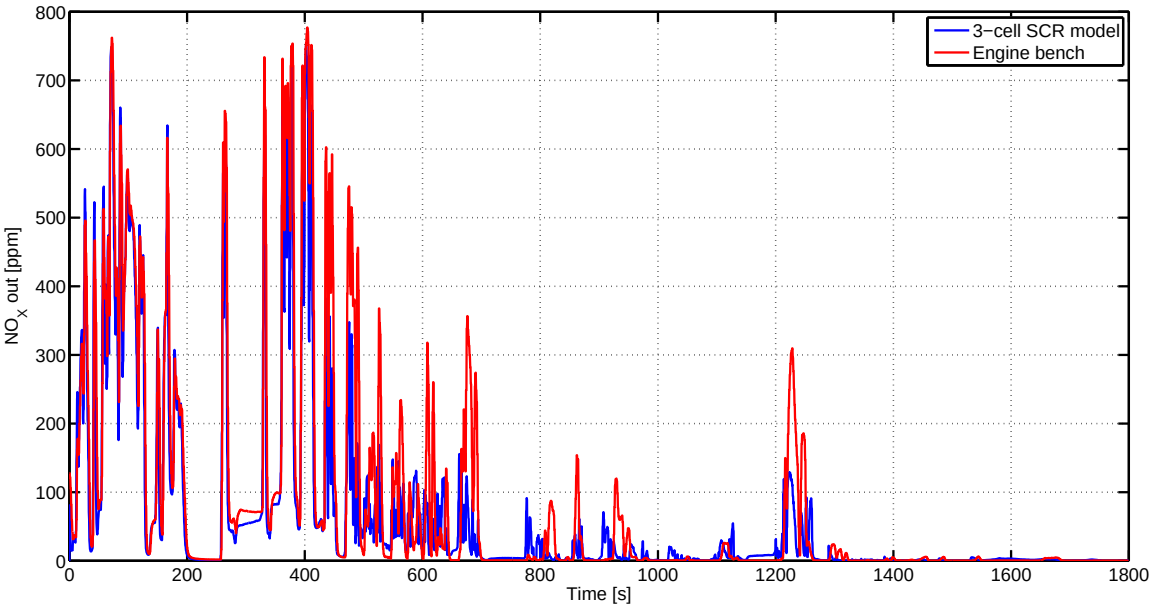

Figure 4.14: SCR out NO_X comparison between 3 cell model and engine bench for the WHTC cycle.

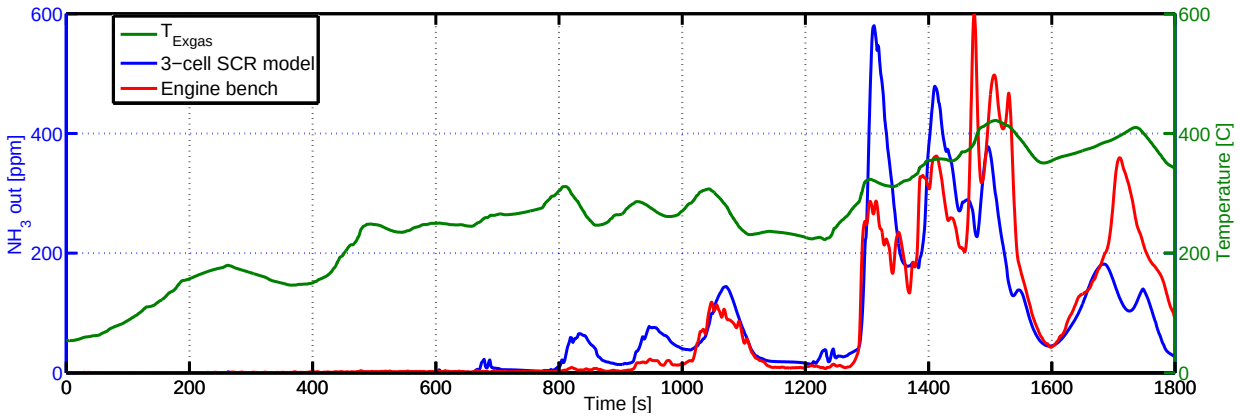

Figure 4.15: SCR out NH_3 comparison between 3 cell model and engine bench for the WHTC cycle.

The correlation between the model and the engine bench data is not perfect due to the following reasons: 1. The test was performed on a fresh catalyst on the engine bench whereas the model parameters were identified for an aged catalyst. 2. The model contains several simplifications.

5

Control strategies

The control strategy adopted is based on the one found in [21]. This model based control strategy consists of a model of an SCR system along with an inversion of that model. An inversion consists of a part of the SCR model which utilizes the equations modelled to back calculate the amount of urea to be injected to maintain a certain set point for NH_3 slip or NO_X/NH_3 ratio.

A schematic diagram of the model along with the inversion is shown below:

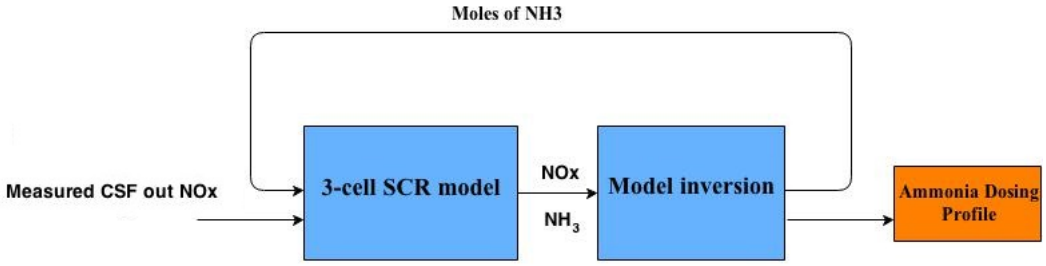

Figure 5.1: Schematic diagram of the feedforward controller

As mentioned above the control strategy developed is implemented offline. Measured engine out NO_X is fed to the feedforward controller. The amount of AdBlue to be injected is calculated from the moles of NH_3 given by the controller as the output. The AdBlue dosing profile is then tested on the engine bench for the same engine out NO_X.

5.1 Control strategy to maintain constant ammonia slip

The control strategy to maintain a constant NH_3 slip is implemented through an inversion of the 3-cell model.

A brief methodology on performing an inversion for a 3-cell model is shown below:

Before carrying out the inversion for the 3-cell model, the equations to calculate the concentrations of NH_3, NO and NO_2 are simplified by replacing a few terms by constants. This is done to gain a better understanding of the inversion only.

Equation 3.13 and 3.16 can be used to obtain the following constants:

$$k_1 = \frac{(\frac{N_{Cell}}{\epsilon.V_c})}{(\frac{R_{ex,gas}}{P_{amb}}).(\frac{N_{Cell}}{\epsilon.V_c}).\dot{m}_{exgas}.T_{cell1} + k_{ads}.C_s.(1-\theta)} \tag{5.1}$$

$$k_2 = \frac{r_{des}}{(\frac{R_{ex,gas}}{P_{amb}}).(\frac{N_{Cell}}{\epsilon.V_c}).\dot{m}_{exgas}.T_{cell1} + k_{ads}.C_s.(1-\theta)} \tag{5.2}$$

$$k_3 = \frac{(\frac{R_{ex,gas}}{P_{amb}}).(\frac{N_{Cell}}{\epsilon.V_c}).\dot{m}_{exgas}.T_{cell1}}{(\frac{R_{ex,gas}}{P_{amb}}).(\frac{N_{Cell}}{\epsilon.V_c}).\dot{m}_{exgas}.T_{cell2} + k_{ads}.C_s.(1-\theta)} \tag{5.3}$$

$$k_4 = \frac{r_{des,cell2}}{(\frac{R_{ex,gas}}{P_{amb}}).(\frac{N_{Cell}}{\epsilon.V_c}).\dot{m}_{exgas}.T_{cell2} + k_{ads}.C_s.(1-\theta)} \tag{5.4}$$

The same can be extended to the concentration equation in the third cell of the model.

$$k_5 = \frac{(\frac{R_{ex,gas}}{P_{amb}}).(\frac{N_{Cell}}{\epsilon.V_c}).\dot{m}_{exgas}.T_{cell2}}{(\frac{R_{ex,gas}}{P_{amb}}).(\frac{N_{Cell}}{\epsilon.V_c}).\dot{m}_{exgas}.T_{cell3} + k_{ads}.C_s.(1-\theta)} \tag{5.5}$$

$$k_6 = \frac{r_{des,cell3}}{(\frac{R_{ex,gas}}{P_{amb}}).(\frac{N_{Cell}}{\epsilon.V_c}).\dot{m}_{exgas}.T_{cell3} + k_{ads}.C_s.(1-\theta)} \tag{5.6}$$

The concentration equations for the three cells can now be written as follows:

$$C_{NH3,1} = k_1.\dot{n}_{\mathrm{NH_3 in}} + k_2 \tag{5.7}$$

$$C_{NH3,2} = k_3.C_{NH3,1} + k_4 \tag{5.8}$$

$$C_{NH3,3} = k_5.C_{NH3,2} + k_6 \tag{5.9}$$

As mentioned earlier, the inversion is a method of working backwards to calculate the amount of NH_3 to be injected. In this case we will work backwards to calculate $\dot{n}_{\mathrm{NH_3},in}$.

Substituting equation 4.8 in equation 4.9, we obtain the following:

$$C_{NH3,3} = k_5.(k_3.C_{NH3,1} + k_4) + k_6 \tag{5.10}$$

Substituting for $C_{\mathrm{NH_3},1}$ in equation in 4.10 we get,

$$C_{NH3,3} = k_5.(k_3.(k_1.\dot{n}_{\mathrm{NH_3 in}} + k_2) + k_4) + k_6 \tag{5.11}$$

Consider 1 mole of exhaust gas. The volume of 1 mole of exhaust gas at NTP can be obtained through the ideal gas relation. The volume of exhaust gas about to exit the SCR which in our case is the volume of exhaust gas about to exit the third cell needs to be calculated. This can be found through the combined gas law as shown below:

$$\frac{P_{amb}.V_{cell3}}{T_{cell3}} = \frac{P_{NTP}.V_{NTP}}{T_{NTP}} \tag{5.12}$$

We express the V_{Cell3} as,

$$V_{cell3} = \frac{1}{Z} = \frac{P_{NTP}.V_{NTP}.T_{cell3}}{T_{NTP}.P_{amb}} \tag{5.13}$$

where Z is a constant used to simplify the expression which will be used in the inversion equation.

We express the concentration of NH_3 leaving the last cell as $C_{\mathrm{NH_3},desired}$ which is taken in ppm. One million parts corresponds to the number of moles of exhaust gas in the convertor. Hence $C_{\mathrm{NH_3},desired}$ ppm of NH_3 corresponds to

$$C_{\mathrm{NH_3}_{desired}}.10^{-6} = \frac{\dot{n}_{\mathrm{NH_3}}}{\dot{n}_{exgas}} \tag{5.14}$$

Dividing equation 4.14 with 4.13 gives the concentration of NH_3 leaving the third cell with respect to the total moles of exhaust gas leaving the convertor. This can be shown as,

$$C_{NH3,3} = \frac{C_{\mathrm{NH_3}_{desired}}.10^{-6}}{V_{cell3}} \tag{5.15}$$

Thus,

$$C_{NH3,3} = C_{\mathrm{NH}_{3desired}}.10^{-6}.Z \tag{5.16}$$

Thus equation 4.11 can be rewritten as,

$$\dot{n}_{\mathrm{NH}_3} = \frac{C_{\mathrm{NH}_{3desired}}.10^{-6}.Z - k_6 - k_5.k_4 - k_5.k_3.k_2}{k_5.k_1.k_3} \tag{5.17}$$

5.2 Control strategy to maintain a constant $\mathbf{NO_X/NH_3}$ ratio

The control strategy to maintain a constant $\mathrm{NO_X/NH_3}$ ratio is implemented through an inversion of the 3-cell SCR model as well.

The procedure to implement a feedforward controller to maintain a constant $\mathrm{NO_X/NH_3}$ ratio can be done in a way similar to the one shown for the constant slip controller shown in the previous section.

We take a ratio $R_{desired}$ which can be expressed as,

$$R_{desired} = \frac{C_{\mathrm{NO_X}}}{C_{\mathrm{NH}_3}} \tag{5.18}$$

If we desire a constant $\mathrm{NO_X/NH_3}$ ratio the amount of $\mathrm{NH_3}$ thats needs to be injected can be expressed as,

$$\dot{n}_{\mathrm{NH}_3} = \frac{\frac{C_{\mathrm{NO_X},cell3}}{R_{desired}} - k_6 - k_5.k_4 - k_5.k_3.k_2}{k_5.k_1.k_3} \tag{5.19}$$

6

Results and discussion

This section will present the results from the engine bench for the various control strategies tested. The dosing profile is generated offline. This gives the urea dosing in g/min sampled at 2 Hz. The tests were carried out on a fresh extruded vanadia based catalyst volume of 11L. The test setup layout is shown in Figure 6.1. T1 to T4 are thermocouples that measure the exhaust gas temperature at various points. R1 to R4 are sampling points for measuring the concentration of various gas species in the exhaust gas. At point R3 which is at the outlet of SCR NO, NO_2, N_2O and NH_3 concentration is measured. At point R4 which is after the ASC all the emissions are measured. The dimension of the various catalysts used in the exhaust line is shown in Table 6.1.

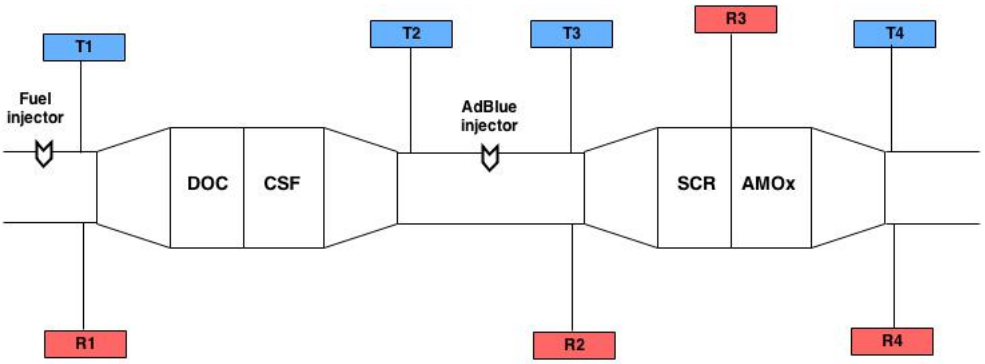

Figure 6.1: Layout of the test setup at the engine bench.

Table 6.1: Catalyst dimensions

Sl no	Catalyst	Dimension
1	DOC	12”x6”
2	CSF	12”x10.5”
3	SCR	10.5”x4”(x2 pcs single leg)
4	ASC	10.5”x2”(x2 pcs single leg)

A range of control strategies from 10 ppm ammonia slip to 200 ppm ammonia slip for a constant slip controller were tested. Control strategies ranged from a ratio of 1.2 to 5 for the constant NO_X to NH_3 ratio controller.

It was found the best results were obtained for the 100 ppm slip controller. The ratio controller

had low slip but the NO_X conversion was not satisfactory.

The engine out and tailpipe emissions are measured during during the 'baseline' test where no urea is dosed. The tail pipe values are used to get the NO_2/NO_X ratio into the SCR. This is under the assumption that there are no further reactions on the SCR or ASC. These measurements serve as the input feed to the controller. The controller is run offline for a set strategy and the dosing profile is obtained at a frequency of 10 Hz.

The dosing profile generated from the controller is fed to the dosing control unit during the engine test. The post SCR NO_X and NH_3 are measured to determine the performance of the controller.

1. **Control strategies for a fresh 11.4L 300 cpsi extruded vanadia catalyst :**

   A number of control strategies were tested on the engine bench for a 11L catalyst. Table 6.2 summarises the different control strategies tested.

   Before the injection of AdBlue for the WHTC cycle a conditioning test and a WHTC cycle with no AdBlue is run. The conditioning test is carried out before each set of control strategies to remove any residual NH_3 that would interfere with the SCR reactions. The conditioning test consists of feeding exhaust gas at a flow rate of 1600 kg/h at 400 °C for an hour. Upon completion of the conditioning test a WHTC run without any ammonia injection is run. The temperature of the SCR after the conditioning test is high. In order to reduce the temperature of the SCR to working temperatures a WHTC cycle is run without any ammonia dosing.

   In all the control strategies the minimum dosing temperature in the controller is set at 175 °C as against a standard of 170 °C used in the flat ANR dosing. The additional 5 degrees acts as a safety margin for the controller during dosing. A minimum torque and minimum speed constraint is also placed on the dosing. The minimum torque limit is 50 Nm and the engine speed is 800 RPM. To summarize the dosing is stopped when any of these constraints are not met.

   Henceforth all strategies named 20.1,21.1 ... so on refer to the first WHTC cycle where the catalyst is empty. 20.2,21.2... refer to the second WHTC cycle and finally 20.3,21.3 refers to the third WHTC cycle. The dosing profile for the first cycle is different from the second cycle as the catalyst is empty in the first cycle. Whereas for the second cycle the ammonia storage is carried over. There is a soak period of 10 minutes at the end of each WHTC cycle where there is no flow of exhaust gas through the catalyst.

   Subscript 1,2,3 and 4 for the 100 PPM slip control denote different dosing profiles. The differences between the different subscripts are found in Table 6.3.

   (a) **Control strategies 28.2 100 PPM_3** This is a constant slip control strategy that targets a constant slip of 100 PPM slip. The results will be presented for the WHTC cycle in different figures given below.

   Figure 6.2 shows the comparison of the NO_X input to the SCR and the SCR out NO_X between the model and the engine bench for the third WHTC cycle. The model captures the dynamics pretty well. The conversion efficiency is 91.8% for the third WHTC cycle.

   Figure 6.3 shows the SCR out ammonia slip from the engine bench and the model. The plot also shows ammonia slip after the ASC and the SCR brick temperature is plotted

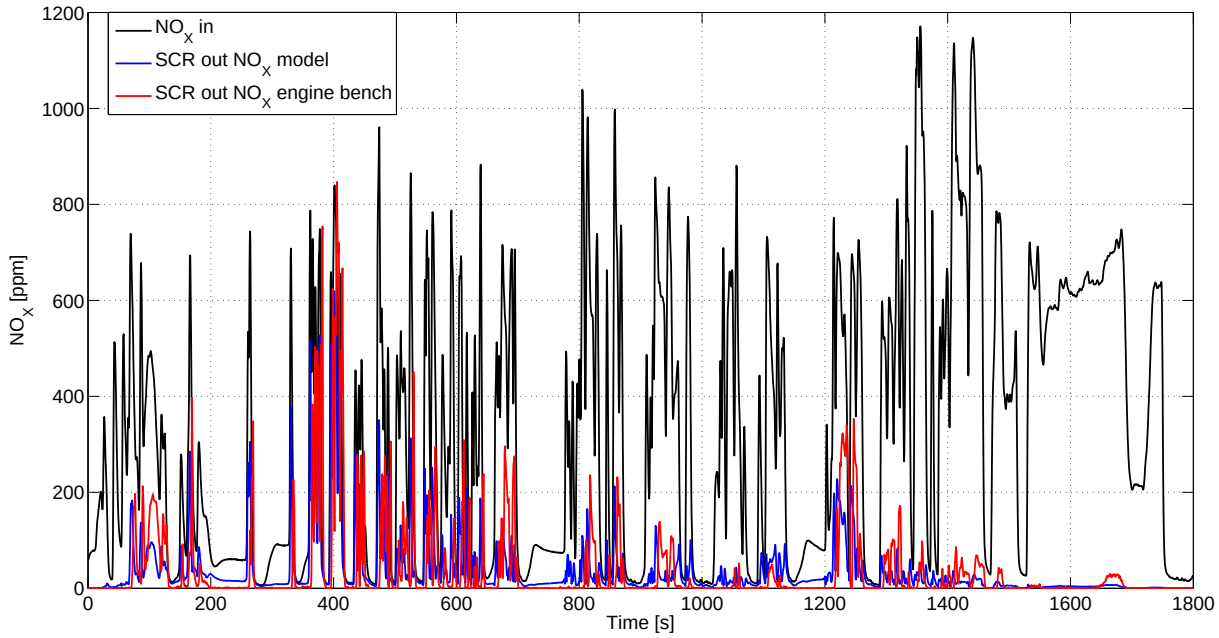

Figure 6.2: Comparison of NO_X in and out of the SCR for 100PPM_3 controller between model and engine bench for the third WHTC cycle. NO_X conversion : 91.8%

against time on the secondary y-axis. The controller tries to maintain a constant slip of 100 ppm whereas the ammonia slip on the engine bench does not correlate to the model very well. The peak ammonia slip downsteam of the SCR is 198 ppm and the peak slip after the ASC is 52 ppm. In order to draw a comparison between flat dosing and the controller the slip from the engine bench for ANR of 1.2 and 1.4 is also included in the same figure. It is clear that the controller reduces the slip drastically compared to the flat ANR. The reasons for discrepancy between slip on the engine bench and model is due to the fact that the 3 cell model was tuned to another model which is not perfect. Secondly the catalyst tested on the engine is a fresh catalyst whereas the model parameters are identified for an aged catalyst.

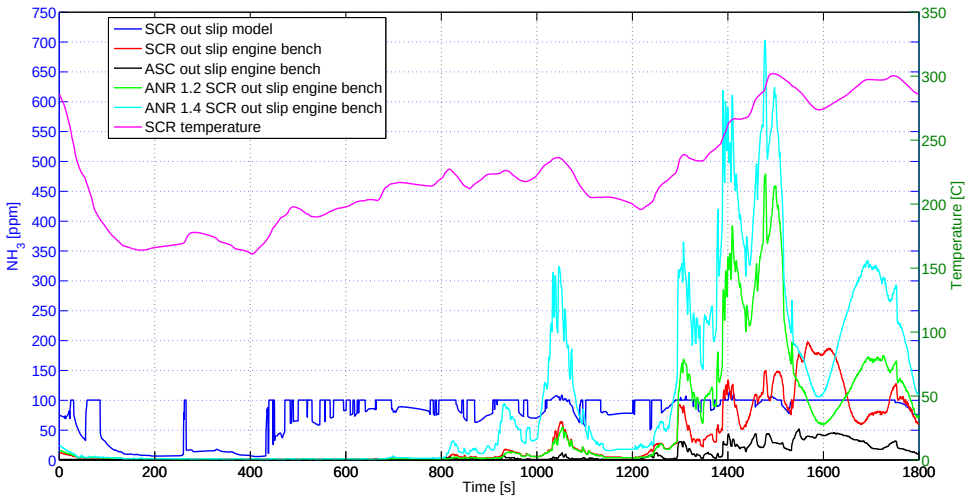

Figure 6.3: Comparison of SCR out ammonia slip between 100 PPM_3 controller, flat ANR 1.2 and 1.4 for the third WHTC cycle. Controller actual ANR : 0.99

Figure 6.4 shows the dosing profile generated by the controller and also the SCR temperature on the secondary y-axis. The standard control problem in an SCR system is during a sharp temperature rise. During a very sharp rise the ammonia that is adsorbed on the surface of the catalyst desorbs and comes out as ammonia slip. From Figure 6.4 it can be seen that the dosing is cut off during a very sharp temperature rise. Such a strategy helps to control the slip during temperature ramps.

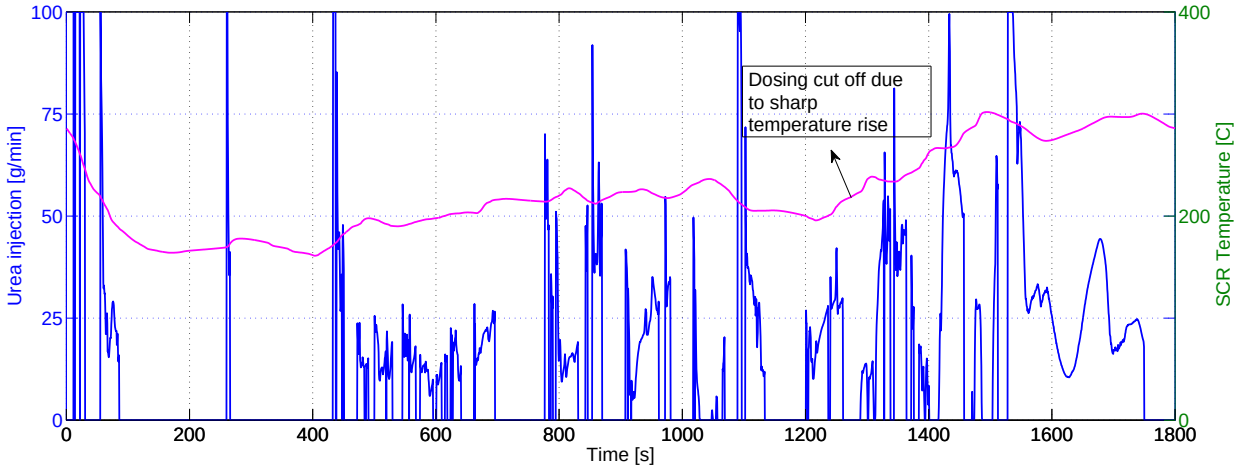

Figure 6.4: Dosing profile, temperature for 100 PPM_3 controller for third WHTC cycle.

Figure 6.5 can be used to further understand the principle behind the working of the controller. It can be seen in the figure that the dosing can be carried out at very high ANR. The controller tries to load the catalyst with a lot of ammonia at favorable temperatures. At other times when the conditions are not suitable, such as sharp temperature rise the dosing is either very low or completely cut off. The lower ANR dosing can be seen in the zoomed in section in the same figure.

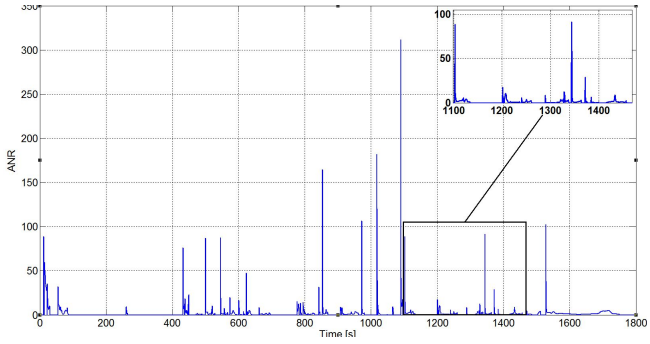

Figure 6.5: ANR for 100 PPM_3 controller for third WHTC cycle.

Figure 6.6 shows the average ammonia fill level in the SCR for first and the second WHTC cycle. It can be seen that at the beginning of the second cycle the fill level is higher when compared to the first cycle, this results in a higher NO_X conversion. After a while it is seen that the fill level overlaps, from here on a similar NO_X conversion can be expected for both the cycles.

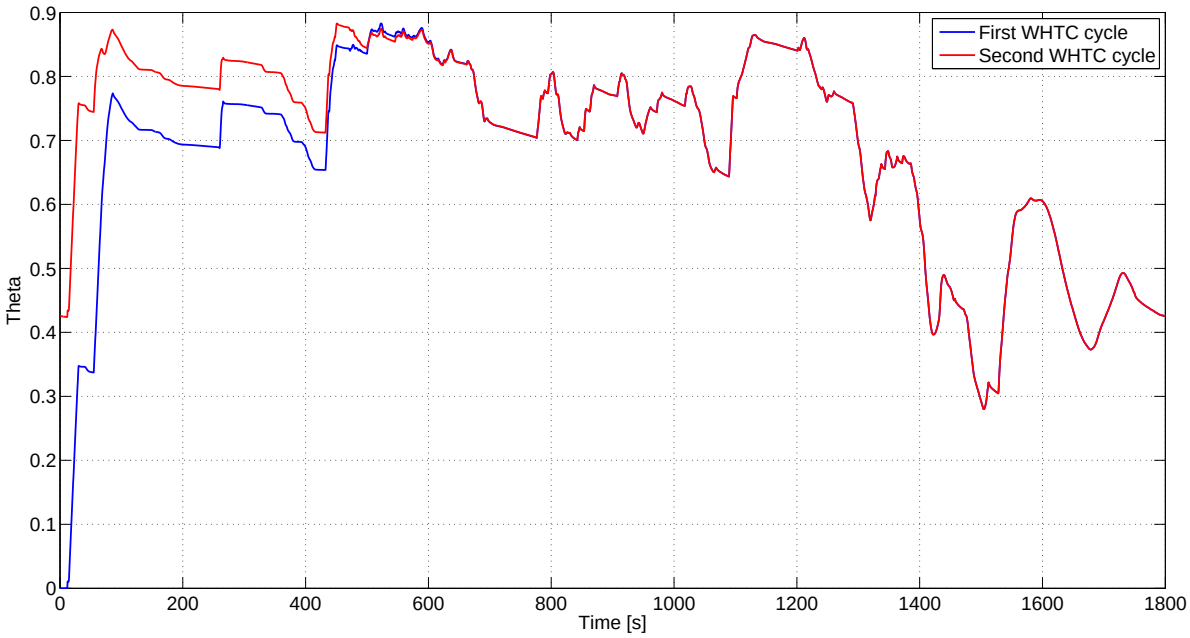

Figure 6.6: Ammonia storage level in the SCR for the first and second WHTC cycle.

(b) **Control strategy 26.2 NO_X to ammonia ratio 1.2 :**
This strategy maintains a constant NO_X to ammonia ratio out of the SCR. The motivation for using such a controller is to have a trade-off between NO_X coming out of the SCR and ammonia slip. The slip controller just considers the ammonia slip whereas the ratio controller considers both the NO_X and ammonia slip. When using the parameters identified to the detailed model, the performance of this controller is not too satisfactory. This is because there is no good correlation of the SCR out NO_X between the model and the engine bench. The model over predicts the SCR out NO_X. The SCR out ammonia slip is under very good control. The model tries to maintain the ratio but on the engine bench this ratio is not maintained. The controller performance can be analysed from the plots shown below.

Figure 6.7 shows the SCR out ammonia slip in the model and engine bench. The plot also shows engine bench ASC out ammonia slip. Peak SCR out ammonia slip is 33 ppm and the average slip is 4 ppm. This strategy has very low slip but this comes at a cost of poor NO_X conversion. With better parameters the ratio controller could perform better. For instantance using the parameters used in strategy 28.1 could yield better results as those parameters are tuned to the engine bench.

Figure 6.8 shows the ANR at different points in the WHTC cycle. Comparing 6.8 to Figure 6.5 it can be seen that the ANR for the ratio controller is much lower than the slip controller. This justifies the lower NO_X conversion of the ratio controller when compared to the slip controller.

Figure 6.9 shows that the controller tries to maintain a ratio of 1.2 where ever possible. In the engine bench this ratio is not achieved as the model does not correlate to the engine bench very well.

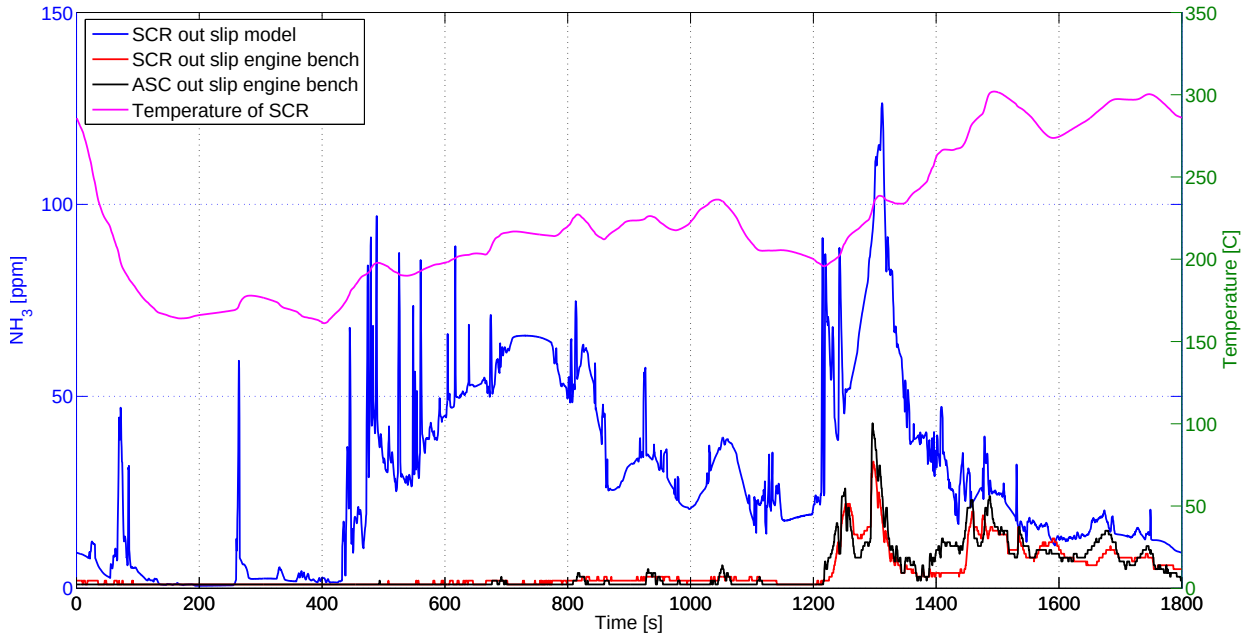

Figure 6.7: Ammonia slip out of the SCR and ASC for Ratio 1.2 controller between model and engine bench for the third WHTC cycle. Average ANR : 0.92

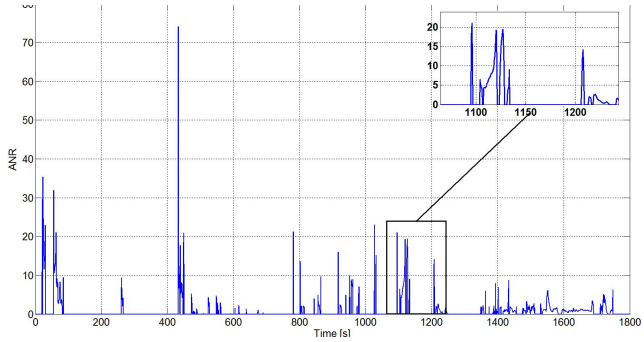

Figure 6.8: ANR for 1.2 Ratio controller for third WHTC cycle.

6.0.1 Comparison of results

This section will compare the results of controller with the flat dosing strategy. The cumulative NO_X in grams and ammonia slip in grams for the first cycle and third cycle of WHTC are used for comparing. Maximum benefit is obtained in the first cycle of the WHTC while using the controller.

Figure 6.10 shows the cumulative NO_X in grams for the various control strategies during the first WHTC cycle. The 100 PPM_3 achieves 23.8 % higher NO_X conversion than a flat ANR 1.4 and 27.5 % higher NO_X conversion than a flat ANR of 1.2. The 100 PPM_1 achieves 19 % higher NO_X conversion than a flat ANR of 1.4 and 22.8 % higher NO_X conversion than a flat ANR of 1.2. The ratio controller does not improve the NO_X conversion. The NO_X conversion drops by 6.5 % when compared to flat ANR of 1.2 and by 11.7 % when compared to a flat ANR of 1.4. It can be seen here that the increase in the NO_X conversion using the slip control strategy is quite significant for the first WHTC cycle.

The benefits are reduced during the second WHTC cycle in terms of NO_X conversion. During the third cycle the 100 PPM_3 achieves 13.8 % higher NO_X conversion than a flat ANR 1.2 and 7 % higher NO_X conversion than a flat ANR of 1.4. The 100 PPM_1 achieves 22.3 % higher NO_X conversion than a flat ANR of 1.2 and 16.2 % higher NO_X conversion than a flat ANR of 1.4. The

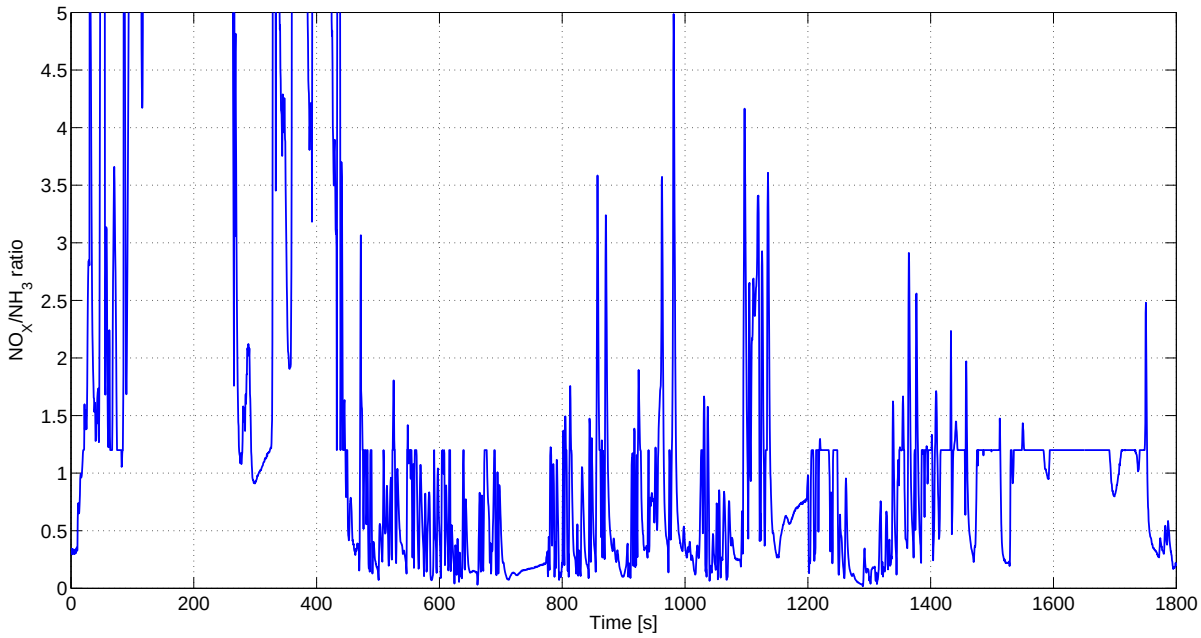

Figure 6.9: SCR out NO_X to ammonia ratio for a ratio 1.2 controller.

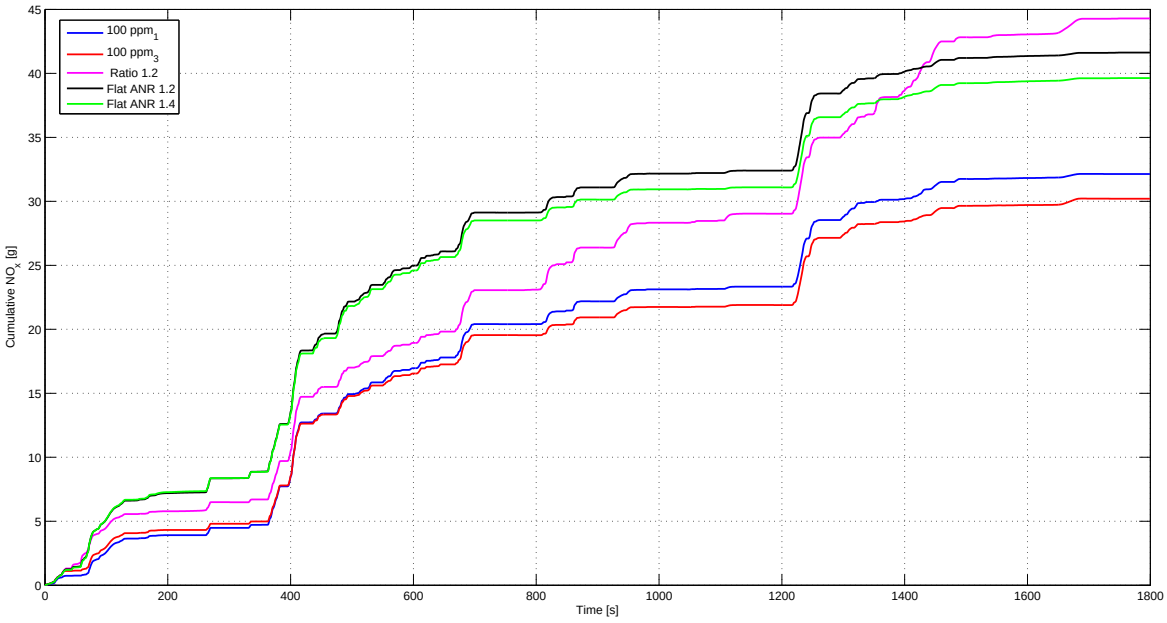

Figure 6.10: Cumulative SCR out NO_X in grams for the various strategies for the first WHTC cycle.

ratio controller once again has a lower NO_X conversion than the flat dosing. The NO_X conversion is 13.5 % lower compared to flat ANR of 1.2 and 22.5 % lower compared to flat ANR of 1.4.

With a control strategy the maximum benefit is seen with the ammonia slip. For the first WHTC cycle 100 PPM_1 reduces the slip by 70 % compared to a flat dosing of ANR 1.4 and 43.7 % less slip compared to a flat ANR of 1.2. The ratio controller barely has any slip. Using the ratio controller the slip is reduced by 97.3 % compared to a flat ANR of 1.4 and by 95 % compared to a flat ANR of 1.2. The results of the cumulative NH_3 slip in grams can be seen in Figure 6.13.

For the third WHTC cycle both the 100 PPM_1 and 100 PPM_3 reduce the slip by 67.8 %

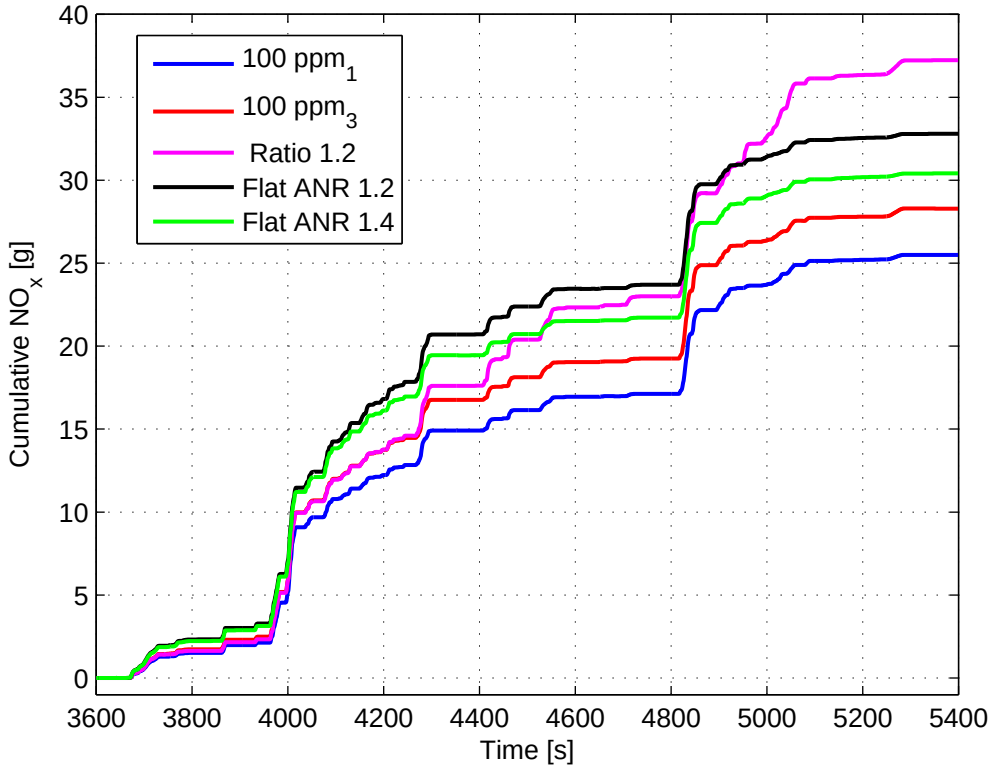

Figure 6.11: Cumulative SCR out NO_X in grams for the various strategies for the third WHTC cycle.

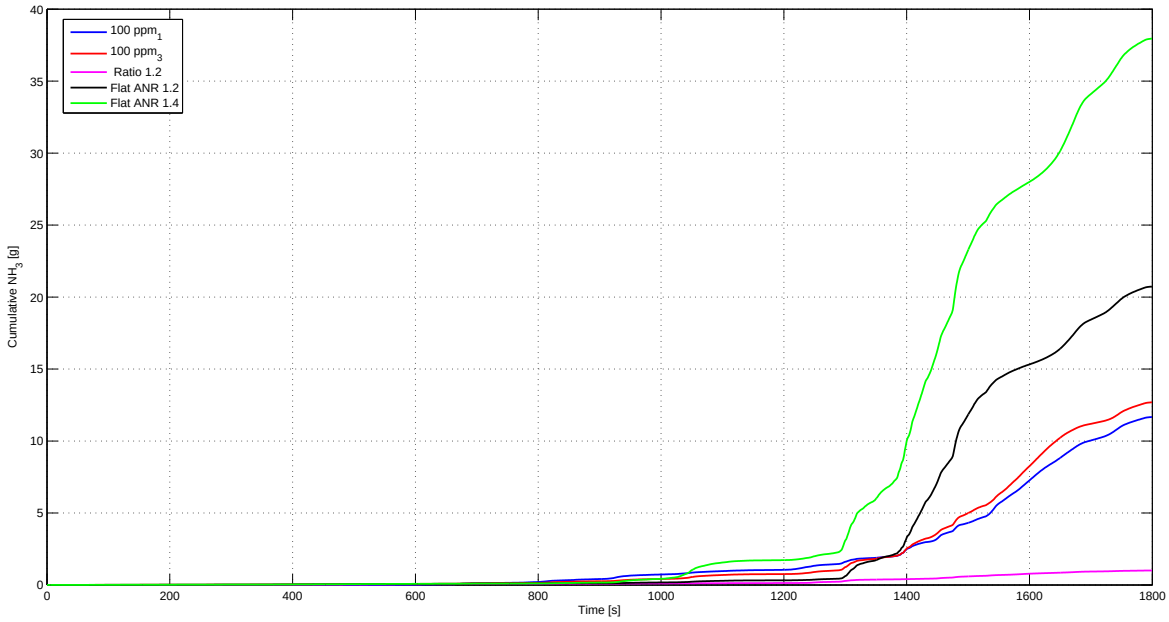

Figure 6.12: Cumulative SCR out NH_3 in grams for the various strategies for the first WHTC cycle.

compared to a flat dosing of ANR 1.4 and 40.7 % less slip compared to a flat ANR of 1.2. The ratio controller barely has any slip. Using the ratio controller the slip is reduced by 95 % compared to a flat ANR of 1.4 and by 92.8 % compared to a flat ANR of 1.2. The results of the cumulative NH_3 slip in grams can be seen in Figure 6.13.

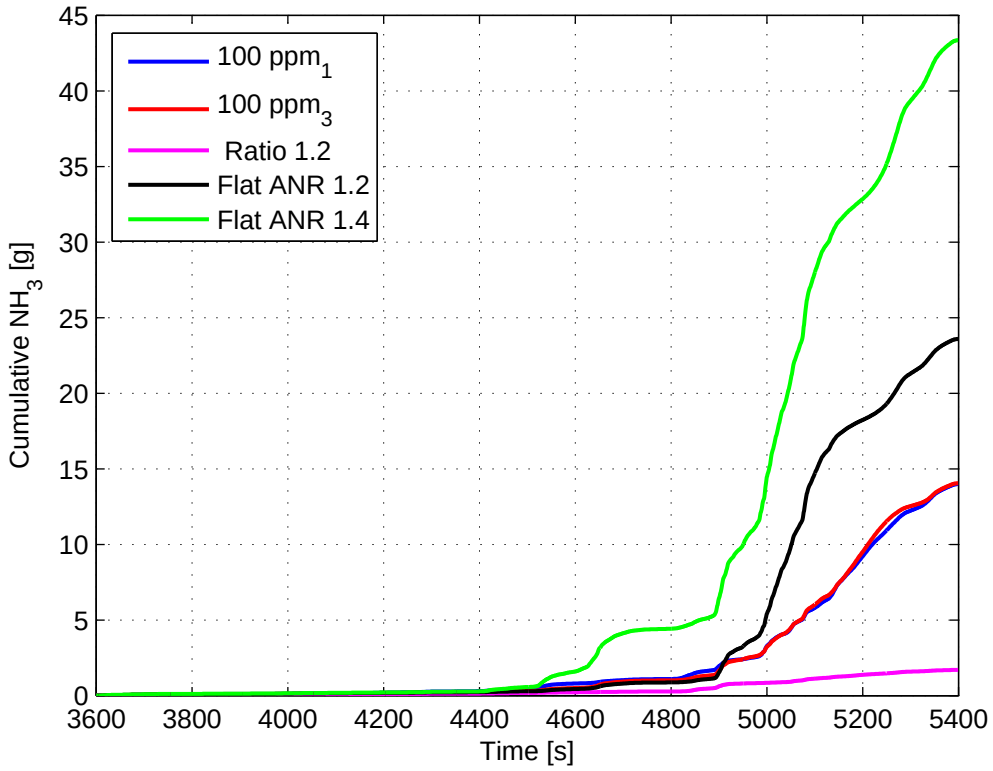

Figure 6.13: Cumulative SCR out NH_3 in grams for the various strategies for the third WHTC cycle.

Table 6.2: Summary of the various control strategies tested on a 11L fresh catalyst

Strategy No	Control Strategy	NO_X conversion [%]	Avg NH_3 slip[ppm]	Actual ANR	Peak NH_3 slip[ppm]	NO_X out engine [g/kWh]	NO_X out tp [g/kWh]
20.1	100 PPM_1	87.9	14	1.09	75	5.671	0.686
20.2	100 PPM_1	91.8	12	1.07	72	5.656	0.466
20.2	100 PPM_1	92.5	15	1.08	91	5.607	0.422
21.1	100 PPM_2	89.1	21	1.17	166	5.640	0.612
21.2	100 PPM_2	92.5	15	1.07	185	5.603	0.423
21.2	100 PPM_2	92.2	18	1.04	195	5.694	0.447
22.1	Ratio 2.5	82.0	3	0.87	19	5.692	1.026
22.2	Ratio 2.5	83.3	3	0.88	24	5.635	0.943
22.2	Ratio 2.5	84.1	4	0.88	35	5.641	0.896
23.1	ANR 1.2	84.1	12	1.03	149	5.694	0.905
23.1	ANR 1.2	90.7	16	1.04	168	5.662	0.528
23.1	ANR 1.2	90.4	16	1.03	167	5.702	0.546
24.1	200 PPM	89.3	31	1.28	161	5.698	0.610
24.2	200 PPM	92.8	38	1.26	194	5.683	0.407
24.2	200 PPM	92.8	46	1.26	239	5.683	0.410
25.1	Ratio 5	83.1	1	0.84	7	5.688	0.962
25.2	Ratio 5	84.0	2	0.85	17	5.643	0.901
25.2	Ratio 5	81.8	2	0.83	10	5.702	1.036
26.1	Ratio 1.2	83.5	2	0.92	15	5.672	0.937
26.2	Ratio 1.2	84.4	3	0.92	26	5.669	0.883
26.2	Ratio 1.2	86.2	4	0.92	43	5.683	0.786
27.1	50 PPM	86.9	5	0.97	27	5.659	0.742
27.2	50 PPM	88.7	6	0.96	30	5.650	0.636
27.2	50 PPM	89.5	9	0.96	47	5.670	0.596
28.1	100 PPM_3	89.0	8	1.06	49	5.679	0.626
28.2	100 PPM_3	91.9	7	0.99	44	5.713	0.464
28.2	100 PPM_3	91.8	9	0.99	52	5.713	0.471
29.1	100 PPM_4	87.8	21	1.13	108	5.696	0.693
29.2	100 PPM_4	90.9	12	1	66	5.678	0.516
29.2	100 PPM_4	91.1	16	1.01	86	5.676	0.505
30.1	150 PPM	86.8	19	1.18	99	5.689	0.749
30.2	150 PPM	92.1	29	1.16	167	5.696	0.448
30.2	150 PPM	92.4	37	1.17	185	5.718	0.436
31.1	ANR 1.4	85.5	26	1.2	246	5.732	0.834
31.1	ANR 1.4	91.3	33	1.2	288	5.731	0.497
31.1	ANR 1.4	91.3	35	1.2	293	5.710	0.499
32.1	ANR 1.1	83.1	8	0.94	104	5.766	0.975
32.1	ANR 1.1	89.0	10	0.94	125	5.754	0.632
32.1	ANR 1.1	89.2	11	0.95	129	5.715	0.615

Table 6.3: Summary of the various control strategies tested on a 11L fresh catalyst

Control Strategy	Definition
100 PPM_1	Parameters identified to the detailed kinetic model
100 PPM_2	Dosing profile from 600 cpsi with a scaled value of capacity
100 PPM_3	Parameters tuned from data obtained from fresh catalyst on engine bench
100 PPM_4	Dosing profile from 600 cpsi with a scaled value of capacity with a manually tuned profile

7

Conclusions

Based on the thesis carried out and the results obtained, the following conclusions can be drawn:

- The NO_X conversion of the constant slip controller relative to the flat dosing strategy is significantly higher as observed in the results obtained. The best performing dosing strategy among the dosing strategies tested is the 100 PPM_3 controller. From Table 6.2 it can be observed that the 100 PPM_3 slip controller uses less urea and achieves a higher NO_X conversion compared to the flat dosing strategies. The NH_3 slip is reduced drastically by using the constant slip controller.
- It can be observed from Figure 6.3 that although the controller maintains the NH_3 slip at the setpoint, the NH_3 slip in the real system is not the same.Since the controller implemented is an open loop controller, the model needs to be very accurate. With better experiments, better parameters can be obtained and the performance of the controller can be significantly improved.
- Although the model of the SCR developed during this thesis was for an extruded vanadia formulation, the SCR model can be easily applied to other catalyst formulations *e.g.* Copper-Zeolite. This would however require that tests be conducted on the chosen formulations to identify the significant chemical kinetics. The model offers flexibility to model additional reactions or remove unnecessary reaction kinetics.
- Best results are obtained when the model is calibrated to engine bench data. However, good measurements are essential.
- The performance of the ratio controller developed was not satisfactory. The main reason for this was poor NO_X predictions from the SCR model. With better predictions, the performance of the ratio controller can be expected to improve.
- The controller is simple enough to be implemented on an ECU.

8

Recommendations and future work

The thesis work carried out has a lot of potential and can be improved upon. Using the control-oriented model of the SCR, various online control strategies can be implemented. In order to realise the potential, a few recommendations are made.

8.1 Parameter estimation

In this thesis, the Johnson Matthey kinetic model was used as a virtual gas bench. Although this provided flexibility and reduced the time taken to carry out experiments a better way to obtain measurement data would be through a real gas bench. Also when calibrating to the engine bench a good set of measurements are needed. In the case of the calibration carried out in this thesis, the SCR inlet temperature measurement was inaccurate. The temperature of the SCR inlet was obtained through a model for heat losses through the exhaust pipe. However there were assumptions regarding the initial temperature of the pipe.

The temperature of the SCR plays a significant role in affecting the reaction kinetics of the SCR. For e.g. if the temperature of the SCR rises earlier compared to the real system, the NH_3 adsorbed on the catalyst desorbs earlier. This in turn causes the NO_X from the SCR to increase as the NO_X conversion decreases. The temperature model of the SCR presented in this thesis was modelled based on a few assumptions. It can be noticed that the heat losses in the SCR of the real system are higher compared to the model. Thus, modelling additional heat losses through the SCR can also improve the NO_X and NH_3 predictions from the model.

In addition to the above mentioned methods it needs to be ensured that any correlation between the parameters is reduced. This can be done through parameter pre-treatment methods such as scaling and centering. For *e.g.* in the rate equation for the desorption, the value of the rate constant and the value of activation energy are multiplied by one another. In this case, the optimization routine might try to increase the value of one parameter and reduce that of another to obtain an optimum.

8.2 Online controller implementation

The control-oriented model of the SCR along with the inversion can be implemented online by using a rapid control prototyping system for *e.g.* dSPACE. The controller can be tested offline and also on the acual system itself. The block diagrams built in simulink can be implemented on the rapid control prototyping system and tested in real time. Such systems behave as an ECU prototype.

However, implementing the feedforward controller online has some limitations. These limitations are:

- Using a feedforward controller to accurately dose the AdBlue requires a very accurate model. In a case where the model deviates considerably from the real system, the performance of the controller will be very poor.
- The performance of the controller during real world operation can be affected by catalyst aging. Once the catalyst ages, the NH_3 storage capacity of the catalyst decreases. If the feedforward controller doses the same amount of AdBlue as it would on a fresh catalyst, there can be very high NH_3 slip.
- In a case where diesel with high sulfur content is used, the SCR can be poisoned by sulfur. This reduces the performance of the SCR catalyst.
- Implementing a complex model online places a significant computational demand on the ECU. The model of the SCR needs to be fast and simple while capturing the essential reaction mechanisms.

A solution to deal with these limitations would be to implement a control strategy with feedback. One way to use feedback in the control strategy would be to use a simple PI element. The feedback signal used can be from a downstream NO_X sensor. The controller input in this case would be the error between the predicted NO_X from the model and the sensor signal. The output from the feedback controller is then used to modify the dosing obtained from the feedforward controller. The use of a feedback controller also ensures that the system is robust to variations in the system.

More advanced feedback control strategies use state-feedback which can also be used effectively for transient operation. In case of a state-feedback control strategy, the surface coverage θ or the AdBlue dosing can be the controller variable. A NH_3 sensor or a NO_X sensor is usually used for this purpose. The feedback signal used is the measured NH_3 from the NH_3 sensor or the measured NO_X from the NO_X sensor. The surface coverage is a quantity that changes with time and is taken as a state in the SCR model. The other states in the SCR model include the concentrations of NO, NO_2 and the temperature.

Any changes in the values of the states at any particular time are corrected using the feedback from the sensors. However θ cannot be measured and is calculated in the model based on any corrections in the concentrations of NO_X or NH_3 downstream. This way, good performance of the controller can be ensured even during transient operation. However, most commercially available NO_X sensors are cross-sensitive to NH_3. The system thus needs to be robust to account for the cross-sensitivity. The cross-sensitivity can be dealt with through signal processing means or by using a mid-brick NH_3 sensor [48]. Dealing with the cross-sensitivity is important as it can induce instability in the feedback loop otherwise.

Controlling the NH_3 surface coverage can provide an ideal combination of low NH_3 slip and high NO_X conversion. However the storage dynamics of the catalyst plays an important role. If the storage capacity of the catalyst is really high *e.g.* in case of Cu-Zeolite, then the dosing system would tend to load the catalyst with a lot of urea. In case of a sharp temperature rise, the stored NH_3 will desorb and this can lead to a large NH_3 slip. Thus, placing a limit on the amount of NH_3 that can be stored at low temperatures is necessary.

An improvement that can be made to the dosing strategy would be to use the temperature information after the turbocharger turbine. Knowing the temperature at the turbine, the dosing can be cut down sooner as the information on the temperature rise is available much before. In the dosing strategy implemented in this thesis, the temperature information at the inlet of the SCR is

utilized to adjust the dosing and place constraints.

To further improvise the constant slip controller, a model of the ammonia slip catalyst can be included. The constant slip controller can be used to maintain a constant NH_3 slip at the outlet of the ammonia slip catalyst. This way, the controller can have a provision to dose even more AdBlue and achieve a higher NO_X conversion.

Bibliography

[1] Stationary internal combustion sources, Tech. rep.
URL http://www.epa.gov/ttnchie1/ap42/ch03/final/c03s03.pdf

[2] NO_X emissions during combustion.
URL http://en.wikipedia.org/wiki/NOx#Prompt

[3] C. Baukal, Everything you need to know about NO_X: Controlling and minimizing pollutant emissions is critical for meeting air quality regulations, Metal finishing 103 (11) (2005) 18–24.

[4] Effects of NO_2 air pollution.
URL http://www.epa.gov/air/nitrogenoxides/

[5] Selective catalytic reduction.
URL http://en.wikipedia.org/wiki/Selective_catalytic_reduction

[6] W.-P. Trautwein, AdBlue as a reducing agent for the decrease of NO_X emissions from diesel engines of commercial vehicles, DGMK, 2003.

[7] Fiat powertrain brochure, Tech. rep.
URL http://www.fptindustrial.com/en-UK/Documents/Brochure/Institutional_EN.pdf

[8] Scania press info: Scania's new Euro-VI range, Tech. rep.
URL http://www.scania.com/Images/wkr0006_tcm40-427362.pdf

[9] I. R. Cloudt, I. R. Baert, I. F. Willems, M. Vergouwe, SCR-only concept for heavy-duty Euro VI applications, MTZ worldwide 70 (9) (2009) 58–63.

[10] Regulatory framework for emissions.
URL https://www.dieselnet.com/standards/eu/hd.php

[11] Anhydrous ammonia health information, Tech. rep.
URL http://www.ndhealth.gov/epr/resources/anhydrous.htm

[12] Diesel exhaust fluid.
URL http://en.wikipedia.org/wiki/Diesel_exhaust_fluid

[13] Diesel systems: Denoxtronic 3.1 – urea dosing system for SCR systems.
URL http://www.boschautomotivetechnology.com/media

[14] L. Guzzella, C. H. Onder, Introduction to modeling and control of internal combustion engine systems, Springer, 2004.
URL http://www.springer.com/engineering/mechanical+engineering/book/978-3-642-10774-0

[15] SCR and fuel efficiency, Tech. rep.
URL http://www.volvotrucks.com/SiteCollectionDocuments/VTNA_Tree/ILF/Products/2010/09-VTM097_FW_SS.pdf

[16] Fuel efficiency, Tech. rep.
URL http://www.brucknertruck.com/pdf/VolvoLiterature/volvo-fuel.pdf

[17] A. Maiboom, X. Tauzia, S. R. Shah, J.-F. Hétet, Experimental study of an LP EGR system on an automotive diesel engine, compared to HP EGR with respect to PM and NO_X emissions and specific fuel consumption, Tech. rep., SAE Technical Paper (2009).

[18] Lean NO_X trap (LNT).
URL http://www.catalysts.basf.com/p02/USWeb-Internet/catalysts/en/content/microsites/catalysts/prods-inds/mobile-emissions/lnt

[19] The collision theory of reaction rates.
URL http://www.chemguide.co.uk/physical/basicrates/introduction.html

[20] KaRE TExT Part II.
URL http://wwwresearch.sens.buffalo.edu/karetext/unit_09/09_Info.pdf

[21] C. M. Schär, Control of a selective catalytic reduction process, Dissertation, Technical Sciences ETH Zürich, No. 15221, 2003, 2003.

[22] M. Devarakonda, G. Parker, J. H. Johnson, V. Strots, S. Santhanam, Model-based estimation and control system development in a urea-SCR aftertreatment system, Tech. rep., SAE Technical Paper (2008).

[23] F. Willems, R. Cloudt, Experimental demonstration of a new model-based SCR control strategy for cleaner heavy-duty diesel engines, Control Systems Technology, IEEE Transactions on 19 (5) (2011) 1305–1313.

[24] F. Willems, R. Cloudt, E. van den Eijnden, M. van Genderen, R. Verbeek, B. de Jager, W. Boomsma, I. van den Heuvel, Is closed-loop SCR control required to meet future emission targets?, Tech. rep., SAE Technical Paper (2007).

[25] A. Stevens, Y. Sun, J. Lian, M. Devarakonda, G. Parker, Optimal SCR control using data-driven models, Tech. rep., SAE Technical Paper (2013).

[26] B. Hollauf, B. Breitsch, T. Sacher, M. Sch, et al., Highest NO_X conversion in SCR catalysts through model based control, Tech. rep., SAE Technical Paper (2011).

[27] T. L. McKinley, A. G. Alleyne, Model predictive control: A unified approach for urea-based SCR systems, Tech. rep., SAE Technical Paper (2010).

[28] WHO adds pressure for stricter Euro-5 standards.
URL http://www.transportenvironment.org/sites/default/files//docs/Bulletin/2006/2006-02_bulletin146_web.pdf

[29] M. Devarakonda, G. Parker, J. H. Johnson, V. Strots, S. Santhanam, Adequacy of reduced order models for model-based control in a urea-SCR aftertreatment system, Tech. rep., SAE Technical Paper (2008).

[30] Adsorption theory.
URL http://en.wikipedia.org/wiki/Adsorption

[31] R. Willi, Low-temperature selective catalytic reduction of NO_X: catalytic behavior and kinetic modeling, Dissertation, Technical Sciences ETH Zürich, No. 11856, 1996, 1996.

[32] C. D. Rakopoulos, E. G. Giakoumis, Diesel engine transient operation, Vol. 5, Springer, 2009.

[33] European stationary cycle, Dieselnet.
URL `https://www.dieselnet.com/standards/cycles/esc.php`

[34] Worldwide Emissions Standards Heavy Duty and Off-Road Vehicles, Delphi, 2011-2012.

[35] World harmonized transient cycle, Dieselnet.
URL `https://www.dieselnet.com/standards/cycles/whtc.php`

[36] J. R. Jernigan, Chemiluminescence NO_X and GFC NDIR CO Analyzers For Low Level Source Monitoring, Thermo Environmental Instruments, 2001.
URL `https://www.thermo.com/eThermo/CMA/PDFs/Various/File_2650.pdf`

[37] A. Elia, C. Di Franco, A. Afzal, N. Cioffi, L. Torsi, Advanced NO_X sensors for mechatronic applications, Triangle Park, NC, USA: InTech.

[38] T. L. McKinley, A. G. Alleyne, C.-F. Lee, Mixture non-uniformity in SCR systems: Modeling and uniformity index requirements for steady-state and transient operation, Tech. rep., SAE Technical Paper (2010).

[39] G. Zheng, G. Palmer, G. Salanta, A. Kotrba, Mixer development for urea SCR applications, Tech. rep., SAE Technical Paper (2009).

[40] E. Samuelsson, S. Holmberg, A CFD study of the urea supply, droplet breakup and mixing in a pipe upstream of a SCR catalyst.

[41] Östen Andersson, Measuring AdBlue quality and understanding requirements of AdBlue infrastructure, 2010.
URL `https://www.integer-research.com/wp-content/uploads/2011/03/25th-9.10-Yara.pdf`

[42] A. Kool, M. Marinussen, H. Blonk, LCI data for the calculation tool feedprint for greenhouse gas emissions of feed production and utilization, Tech. rep. (2012).
URL `https://www.blonkconsultants.nl/upload/pdf/PDV%20rapporten/fertilizer_production%20D03.pdf`

[43] C. Lambert, R. Hammerle, R. McGill, M. Khair, C. Sharp, Technical advantages of urea SCR for light-duty and heavy-duty diesel vehicle applications, Tech. rep., SAE Technical Paper (2004).

[44] Y. Niki, K. Hirata, T. Kishi, T. Tsukamoto, Y. Ichikawa, Y. Nitta, D.-H. Yoo, Evaluation of NO_X reduction performance and slipped NH_3 of SCR system with one-dimensional SCR simulation.

[45] L. Eriksson, Mean Value Models for Exhaust System Temperatures, SAE Technical Paper Series, 2002.

[46] Fminsearchbnd.
URL `http://www.mathworks.com/matlabcentral/fileexchange/8277-fminsearchbnd--fminsearchcon`

[47] Z. Lin, Sensitivity Analysis of SWAT Using SENSAN.
URL `http://www.ndsu.edu/pubweb/~zhulin/pdf/teaching/sensitivity%20analysis.pdf`

[48] P. Chavannavar, Development and implementation of a mapless, model based SCR control system, Tech. rep., SAE Technical Paper (2014).